Accepted Manuscript

Design, synthesis and biological activities of 2,3-dihydroquinazolin-4(1*H*)-one derivatives as TRPM2 inhibitors

Han Zhang, Huan Liu, Xiao Luo, Yuxi Wang, Yuan Liu, Hongwei Jin, Zhenming Liu, Wei Yang, Peilin Yu, Liangren Zhang, Lihe Zhang

PII: S0223-5234(18)30385-4

DOI: 10.1016/j.ejmech.2018.04.045

Reference: EJMECH 10394

To appear in: *European Journal of Medicinal Chemistry*

Received Date: 31 January 2018

Revised Date: 6 April 2018

Accepted Date: 21 April 2018

Please cite this article as: H. Zhang, H. Liu, X. Luo, Y. Wang, Y. Liu, H. Jin, Z. Liu, W. Yang, P. Yu, L. Zhang, L. Zhang, Design, synthesis and biological activities of 2,3-dihydroquinazolin-4(1*H*)-one derivatives as TRPM2 inhibitors, *European Journal of Medicinal Chemistry* (2018), doi: 10.1016/j.ejmech.2018.04.045.

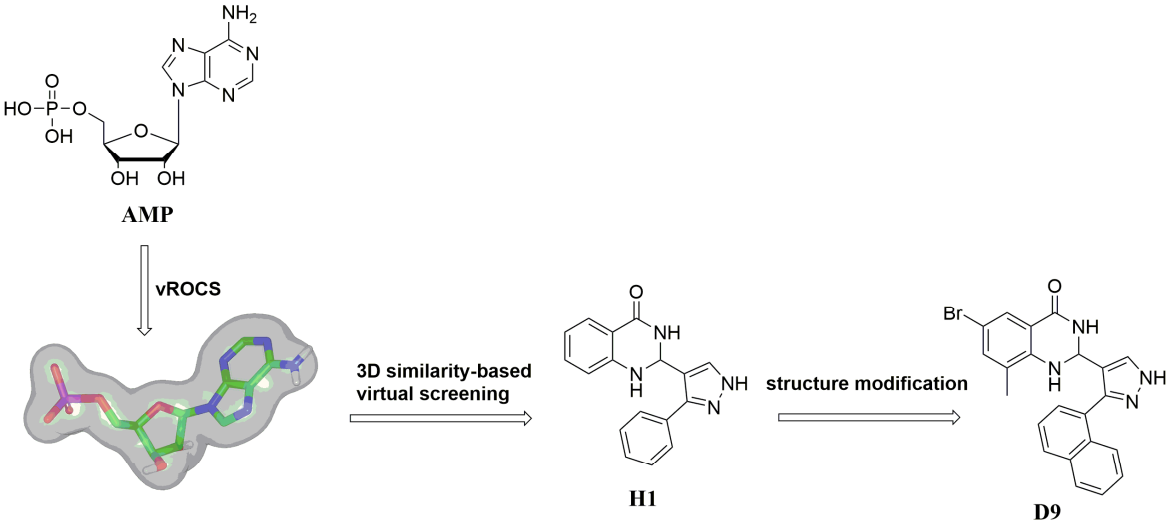

Design, synthesis and biological activities of 2,3-dihydroquinazolin-4(1*H*)-one derivatives as TRPM2 inhibitors

Han Zhang [a1], Huan Liu [b1], Xiao Luo [a], Yuxi Wang [a], Yuan Liu [a], Hongwei Jin [a], Zhenming Liu [a], Wei Yang [b], Peilin Yu [c*], Liangren Zhang [a*], Lihe Zhang [a]

[a] *State Key Laboratory of Natural and Biomimetic Drugs, School of Pharmaceutical Sciences, Peking University, Beijing 100191, PR China*

[b] *Department of Neurobiology, Key Laboratory of Medical Neurobiology of the Ministry of Health of China, Zhejiang University School of Medicine, Hangzhou, Zhejiang 310058, P. R. China*

[c] *Department of Toxicology, School of Public Health, Zhejiang University, Hangzhou, Zhejiang 310058, P. R. China*

[*] Corresponding authors:

E-mail: liangren@bjmu.edu.cn or yupeilin@zju.edu.cn

[1] These authors contributed to the work equally.

Abstract

Transient receptor potential melastatin 2 (TRPM2), a Ca^{2+}-permeable cationic channel, plays critical roles in insulin release, cytokine production, body temperature regulation and cell death as a reactive oxygen species (ROS) and temperature sensor. However, few TRPM2 inhibitors have been reported, especially TRP-subtype selective inhibitors, which hampers the investigation and validation of TRPM2 as a drug target. To discover novel TRPM2 inhibitors, 3D similarity-based virtual screening method was employed, by which 2,3-dihydroquinazolin-4(1*H*)-one derivative **H1** was identified as a TRPM2 inhibitor. A series of novel 2,3-dihydroquinazolin-4(1*H*)-one derivatives were subsequently synthesized and characterized. Their inhibitory activities against the TRPM2 channel were evaluated by calcium imaging and electrophysiology approaches. Some of the compounds exhibited significant inhibitory activity, especially **D9** which showed an IC_{50} of 3.7 μM against TRPM2 and did not affect the TRPM8 channel. The summarized structure-activity relationship (SAR) provides valuable insights for further development of specific TRPM2 targeted inhibitors.

Key words:

TRPM2; 2,3-dihydroquinazolin-4(1*H*)-ones; inhibitors; SAR; virtual screening

1. Introduction

Transient receptor potential (TRP) channels belong to a novel family of cationic ion channels with strong impacts on cellular functions and signaling pathways [1]. The mammalian TRP channel superfamily is composed of 28 members that are grouped into six subfamilies based on their homology of amino acid sequences [2,3]. Transient receptor potential melastatin (TRPM), a subfamily of TRP channels, contains eight subtypes that can be divided into four pairs based on their homology: TRPM1/TRPM3; TRPM2/TRPM8; TRPM4/TRPM5 and TRPM6/TRPM7 [4]. The TRPM2 channel is a multifunctional nonselective cation channel that is expressed in a range of tissues including brain, bone marrow, spleen, heart, liver and lung [2,4]. As a ROS sensor, TRPM2 plays important roles in a variety of cells, contributing to cellular functions including insulin release, cytokine production, cell motility, endothelial hyperpermeability and cell death [5,6]. Moreover, it also functions as an important temperature sensor in a subpopulation of hypothalamic neurons, monitoring internal body temperature [7,8]. Therefore, the TRPM2 channel has been reported to be involved in many pathological processes such as ischemia/reperfusion injury [9], diabetes [10], neurodegeneration [11], cardiovascular diseases [12] and chronic inflammation [5,13]. Mice knockout studies have shown that inhibition of TRPM2 reduced CA1 pyramidal neuronal death and memory impairment in a bilateral common carotid artery occlusion (BCCAO) model [14], reduced inflammatory markers in bleomycin-induced lung inflammation [13], and attenuated inflammatory and neuropathic pain in various pain models [15]. Therefore, development of TRPM2 inhibitors will not only provide direct molecular tools for the pharmacological researches related to this channel, but also lead to therapeutic advances for diseases mediated by this channel.

Activation of the TRPM2 channel has been widely studied, which provides us information for the design of its inhibitors. The C terminus of TRPM2 channel has a NUDT9 homology (NUDT9-H) domain that is homologous to the NUDT9 adenosine diphosphate ribose (ADPR) hydrolase (~50% similarity) [6]. And the TRPM2 channel has been proved to be primarily activated by binding of ADPR to the NUDT9-H domain [16], of which the binding pocket has been revealed by one of our recent work [17]. Besides, as a redox-sensitive channel, TRPM2 can also be activated by agents that produce reactive oxygen species (ROS) such as hydrogen peroxide (H_2O_2), although the mechanism of action remains debatable [18].

Several TRPM2 inhibitors have been reported with inhibitory activities at micromolar levels, among which are imidazole or anthranilic acid derivatives, such as econazole, clotrimazole [19], flufenamic acid (FFA) [20,21], 2-(3-methylphenyl) aminobenzoic acid (3-MFA) [21], N-(*p*-amylcinnamoyl) anthranilic acid (ACA) [22] and 2-aminoethoxydiphenyl borate (2-APB) [23] (Fig. 1). However, most of these compounds lack specificity, especially considering that the TRPM8

channel has high homology with TRPM2. For instance, although 20 μM ACA completely blocked both ADPR-induced whole-cell currents and H_2O_2-induced Ca^{2+} signals (IC_{50} = 1.7 μM) in HEK293 cells transfected with human TRPM2, it also blocked the TRPM8 channel with an IC_{50} value of 3.9 μM (Ca^{2+} signals) [22]. In addition, several nucleotide analogues (Fig. 1) such as AMP [24,25], 8-bromoadenosine 5′-diphosphoribose (8-Br-ADPR) [26] and a series of synthesized ADPR analogues (i.e., 8-phenyl-2′-*deoxy*-ADPR and our recently discovered compound **8a**) [27,28] have also been reported as TRPM2 inhibitors. They usually function as competitive inhibitors to block the binding of ADPR to NUDT9-H domain [24-26]. For instance, AMP inhibits TRPM2-mediated currents with an IC_{50} of about 70 μM as a negative feedback regulator [6,24,25]. Although these nucleotide analogues are thought to selectively inhibit TRPM2, due to multiple hydroxyl groups and negatively charged pyrophosphate group, its poor membrane permeability limited their application [28,29]. Recently, scalaradial was identified as the active component in an extract of *Cacospongia* that showed strong TRPM2 inhibitory activity, but it was an indirect effect on the channel [30]. Therefore, discovery of novel TRPM2 inhibitors is required to better understand the channel functions and for the potential therapeutic development of this class of agents.

3D similarity-based virtual screening is one of the ligand-based virtual screening (LBVS) methods, which has resulted in the identification of many active compounds in drug discovery programs [31]. In this study, AMP was used as the query structure in 3D similarity-based virtual screening method to achieve scaffold hopping. As a result, 2,3-dihydroquinazolin-4(1*H*)-one derivative **H1** was discovered to be a novel TRPM2 inhibitor. A variety of **H1** derivatives were further designed by modification of substituted groups or positions on the scaffold to elucidate the structure-activity relationship (SAR) and discover the most active compounds. The TRPM2 inhibitory activities of all synthesized compounds were assessed by calcium imaging and electrophysiology approaches. In addition, the inhibitory activities of the most active compounds against TRPM8 were also evaluated. Herein, we report the synthesis and biological investigation of these compounds, which will definitely promote the discovery of novel specific TRPM2 inhibitors.

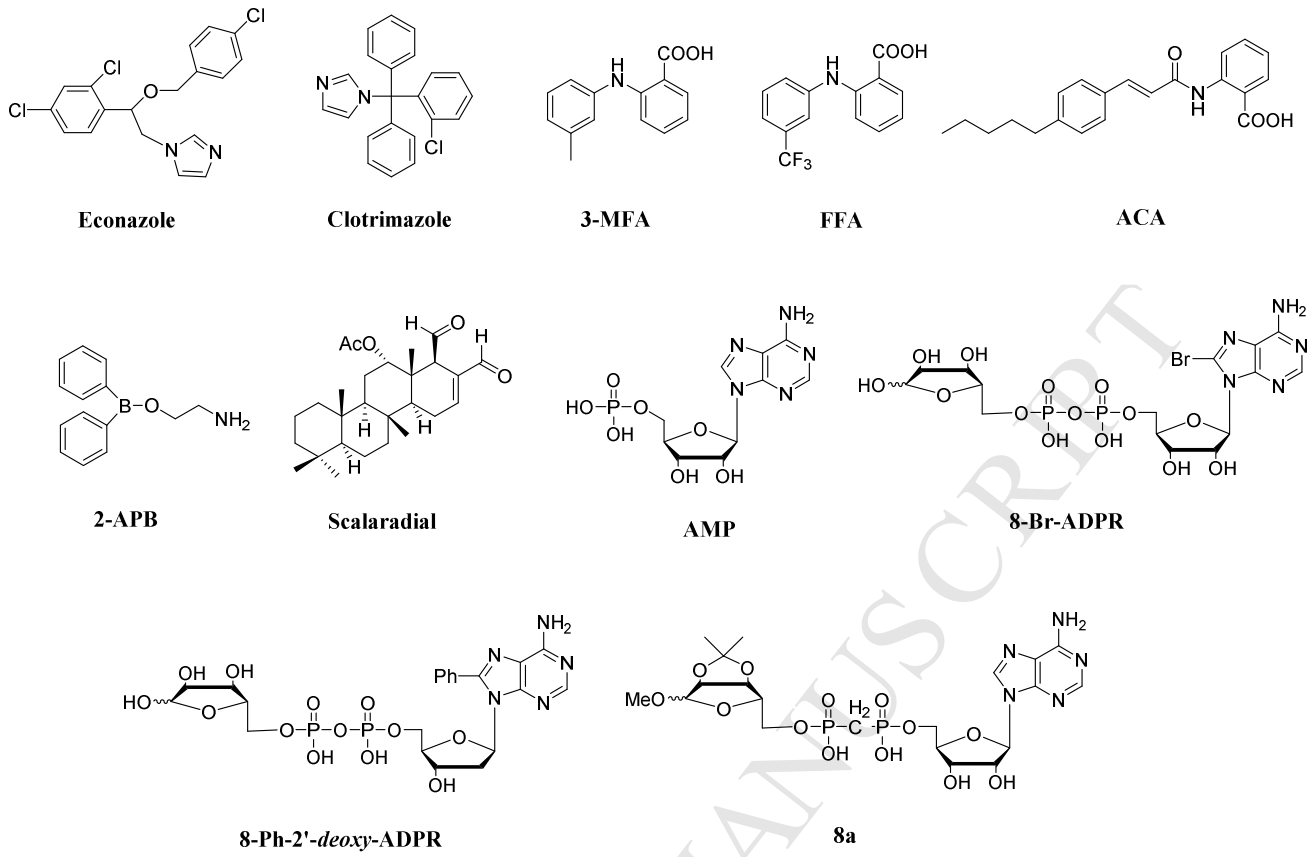

Fig. 1. Chemical structures of some TRPM2 inhibitors.

2. Results and discussion

2.1. Virtual screening and biological evaluation

In an effort to discover novel inhibitors of TRPM2, 3D shape- and electrostatic-based similarity virtual screening approaches were employed (Fig. 2A). The optimized conformation of AMP (Fig. 2B) was used as query to search SPECS (http://www.specs.net/) and PKU_CNCL (http://www.pkucncl.cn/) databases by ROCS 3.1.2 (OpenEye Scientific Software, Inc) program. As a result, the top 3,000 compounds were retained based on 'Shape Tanimoto' score in each structure. EON 2.1.0 (OpenEye Scientific Software, Inc) was then employed to calculate the electrostatic distribution similarity of the retained compounds according to the original query, and the top 300 compounds were retained based on the 'ET_pb' score in each structure. In the end, 600 compounds were clustered and visually inspected. After the synthetic feasibility was evaluated, 24 compounds (Fig. S1, Table S1) were selected for biological evaluation.

Fluorescent calcium imaging was used to preliminarily evaluate the inhibitory activities of

these 24 compounds in HEK293 cells stably expressing human TRPM2. After incubated with cells for 30 min at a concentration of 30 μM, compounds **H1** and **H18** significantly reduced H_2O_2-induced Ca^{2+} fluorescence increase (Fig. S2). Whole-cell patch-clamp recordings were then performed on **H1** to further validate its inhibitory activity. When added intracellularly and simultaneously with 500 μM ADPR, **H1** showed no inhibition on ADPR induced TRPM2 currents at either low (30 μM) or high (1 mM) concentrations (Fig. S3). In contrast, extracellular addition of **H1** at 30 μM resulted in a reduction of TRPM2 current by 55% (Fig. S4). These results indicated **H1** was a novel extracellular inhibitor of the TRPM2 channel.

AMP is one of the hydrolysis products of ADPR, and potentially represents an autoregulatory negative feedback mechanism of TRPM2 activity. The inhibitory activity of AMP is thought to be the result of a competition for the NUDT9-H domain [24,25]. Since **H1** was identified by 3D similarity virtual screening based on AMP structure, it should in theory have a similar mode of action as AMP that acts at the intracellular NUDT9-H domain. However, **H1** only inhibits the TRPM2 current extracellularly, which led us to hypothesize that there are also extracellular binding sites for AMP on the TRPM2 channel. Thus, whole-cell patch-clamp recordings were used to investigate this hypothesis. A concentration-dependent extracellular inhibition by AMP on the TRPM2 currents was indeed observed (Fig. S5).

Previous studies including ours indicated several metals or compounds inhibited TRPM2 activity through the extracellular pore region of TRPM2 [32-34]. Considering that H995A is a key residue involved in several metals induced TRPM2 inhibition or inactivation, while D964A has no effect on TRPM2 function. To determine whether **H1** and AMP interacted with the extracellular pore region of the TRPM2 channel, we detected the effects of **H1** and AMP on mutants of these two residues as previously described [32]. Similar to wild-type (WT) TRPM2 channel, the inhibition by **H1** for the D964A mutant was rapid and about 50%. In contrast, in cells expressing the H995A mutant channel, substantial inhibition did not occur in response to extracellular **H1** over several minutes (Fig. 2D). On average, **H1** resulted in a reduction of ADPR-induced currents by 40 % and 4 % for the D964A and H995A mutant channel, respectively. Residual currents were abolished by subsequent application of pH = 5. We also tested the inhibitory effect of AMP in the D964A and H995A mutant channels, and it was similar to that of **H1** (Fig. 2E). These results implied that the His^{995} residue was an important molecular determinant conferring on the TRPM2 channel the

sensitivity to inhibition by extracellular AMP and **H1**, suggesting that both these two compounds shared the same mechanism in inhibiting TRPM2 through interacting with the extracellular pore region.

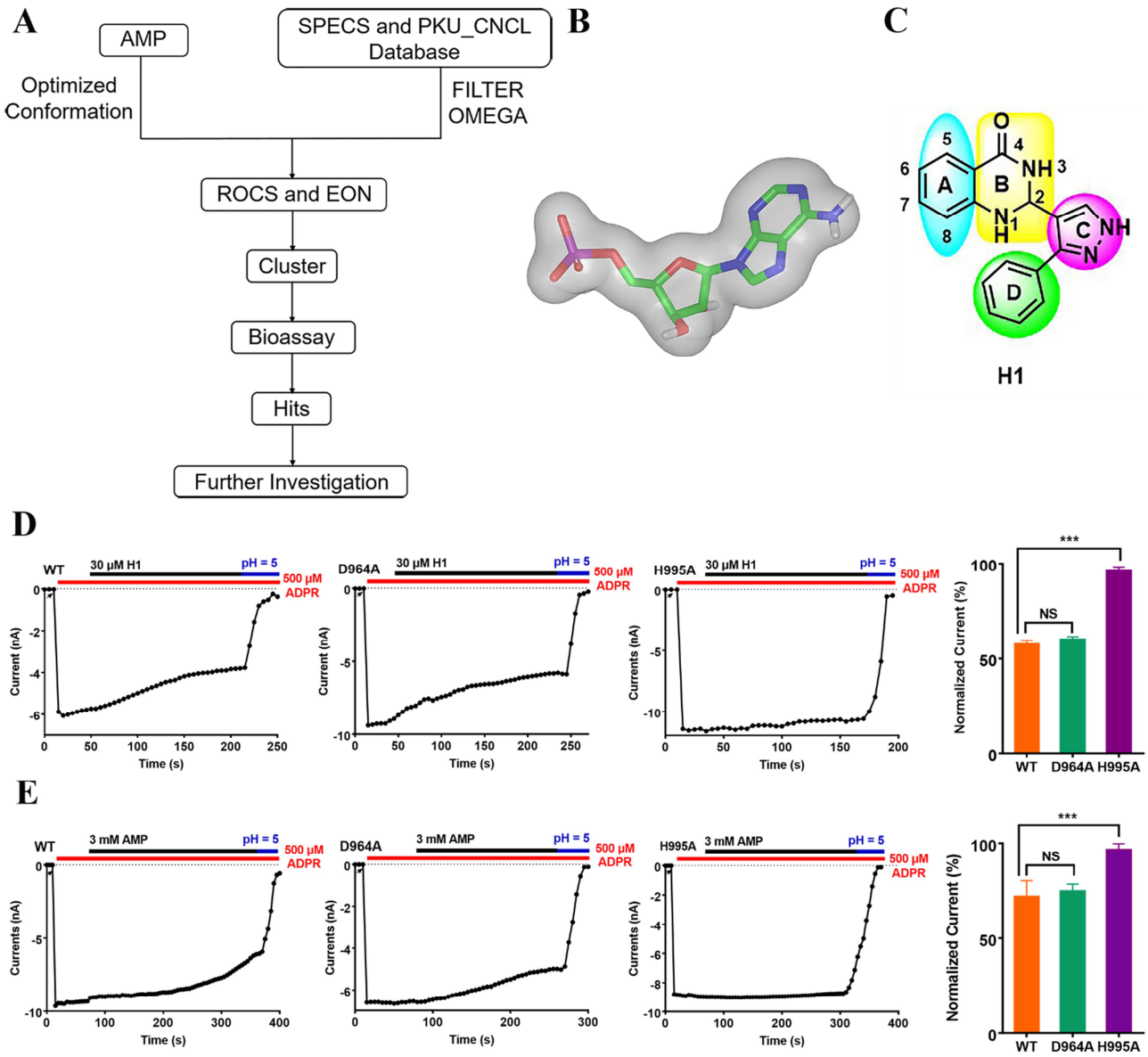

Fig. 2. 3D similarity-based virtual screening and inhibition of the TRPM2 current by **H1** in HEK293 cells stably expressing human TRPM2. (A) Flow chart illustrating the virtual screening process. (B) The ROCS query generated from optimized conformation of AMP. (C) Chemical structure of **H1** is divided into four moieties according to different rings. (D) and (E) Representative 500 μM ADPR-induced currents for WT or indicated mutants with extracellular treatment of **H1** and AMP in whole-cell electrophysiology recordings. Data were presented as mean ± SEM from six independent experiments (n = 6), and NS were presented as no significant difference for indicated comparisons, ***$P < 0.005$.

2.2. Chemistry

Further structural optimizations were performed on **H1** to discover more active extracellular inhibitors of the TRPM2 channel. Starting from the molecular structure of **H1**, we divided **H1** into four moieties A, B, C and D according to the different rings for structural modifications (Fig. 2C). The general synthetic routes for preparation of **H1**, **Class A**, **B**, **C** and **D** are described in Scheme 1-Scheme 9.

Treatment of anthranilic acids (**1a-1q, 1w, 1x)** with EDC•HCl and NH_4Cl or methyl anthranilates (**2r-2v)** with NH_3•H_2O afforded anthranilic diamides (**3a-3x)** [35]. Compounds **H1**, **A1**–**A23** were obtained at 45%–67% yields from **3a–3x** and commercially available 3-phenyl-1*H*-pyrazole-4-carbaldehyde (**4a)** through cyclocondensation reaction under the catalysis of cyanuric chloride (Scheme 1, Scheme 2) [36].

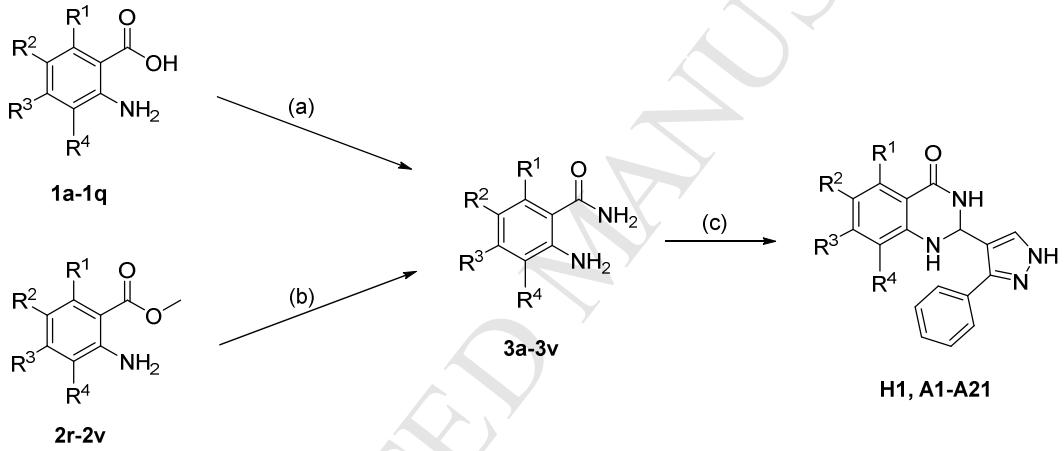

1a, 3a, H1: R^1 = H, R^2 = H, R^3 = H, R^4 = H
1b, 3b, A1: R^1 = H, R^2 = Cl, R^3 = H, R^4 = CH_3
1c, 3c, A2: R^1 = H, R^2 = Cl, R^3 = H, R^4 = H
1d, 3d, A3: R^1 = H, R^2 = CH_3, R^3 = H, R^4 = CH_3
1e, 3e, A4: R^1 = Cl, R^2 = H, R^3 = H, R^4 = H
1f, 3f, A5: R^1 = CH_3, R^2 = H, R^3 = H, R^4 = H
1g, 3g, A6: R^1 = H, R^2 = H, R^3 = H, R^4 = Br
1h, 3h, A7: R^1 = H, R^2 = H, R^3 = H, R^4 = NO_2
1i, 3i, A8: R^1 = H, R^2 = F, R^3 = H, R^4 = CH_3
1j, 3j, A9: R^1 = H, R^2 = Cl, R^3 = H, R^4 = Cl
1k, 3k, A10: R^1 = H, R^2 = Br, R^3 = H, R^4 = CH_3
1l, 3l, A11: R^1 = H, R^2 = Br, R^3 = H, R^4 = OCH_3
1m, 3m, A12: R^1 = H, R^2 = CH_3, R^3 = H, R^4 = Br
1n, 3n, A13: R^1 = H, R^2 = F, R^3 = H, R^4 = F
1o, 3o, A14: R^1 = H, R^2 = F, R^3 = H, R^4 = Br
1p, 3p, A15: R^1 = H, R^2 = I, R^3 = H, R^4 = I
1q, 3q, A16: R^1 = H, R^2 = I, R^3 = H, R^4 = CH_3
2r, 3r, A17: R^1 = H, R^2 = H, R^3 = H, R^4 = CH_3
2s, 3s, A18: R^1 = H, R^2 = Cl, R^3 = H, R^4 = I
2t, 3t, A19: R^1 = H, R^2 = H, R^3 = Br, R^4 = H
2u, 3u, A20: R^1 = H, R^2 = Br, R^3 = H, R^4 = Br
2v, 3v, A21: R^1 = H, R^2 = F, R^3 = H, R^4 = H

Scheme 1. Synthesis of compounds **H1**, **A1–A21**. Reagents and conditions: (a). EDC•HCl, HOBt, NH_4Cl, DIPEA, DMSO, r.t., 15 h; (b). NH_3•H_2O, 100 °C, 12 h; (c). **4a**, cyanuric chloride, CH_3CN, MeOH or DMSO, r.t., 0.5-2 h.

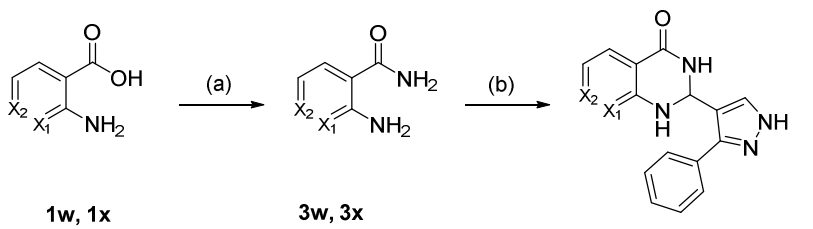

Scheme 2. Synthesis of compounds **A22, A23**. Reagents and conditions: (a). EDC•HCl, HOBt, NH_4Cl, DIPEA, DMSO, r.t., 15 h; (b). **4a**, cyanuric chloride, DMSO, r.t., 0.5-2 h.

Cyclocondensation reactions were accomplished from **4a** and **5a** or **5b** by the catalysis of 2-morpholinoethanesulfonic acid in aqueous 50% ethanol to form compounds **A24** or **A25**, respectively (Scheme 3) [37].

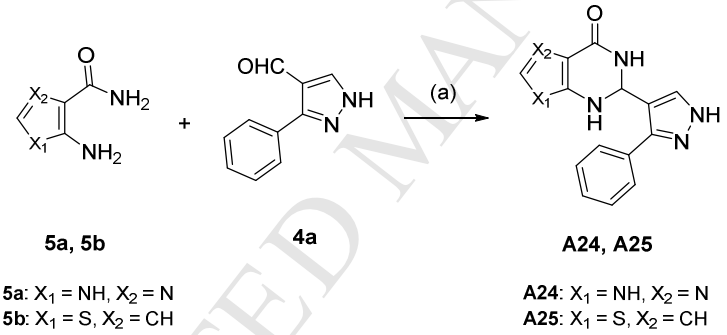

Scheme 3. Synthesis of compounds **A24, A25**. Reagents and conditions: (a). 2-morpholinoethanesulfonic acid, 50 % EtOH (aq), 60 °C, 3 h.

2-Aminobenzenesulfonamide (**6)** was reacted with **4a** or **4e** in the presence of Amberlyst-15 under ultrasound irradiation (40 KHz) to afford compounds **B1** or **B2**, respectively (Scheme 4) [38].

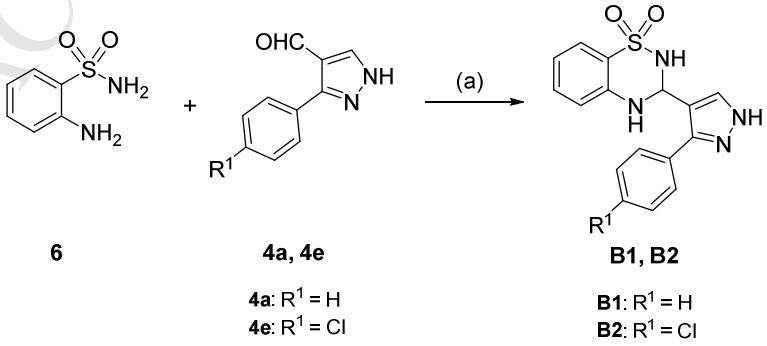

Scheme 4. Synthesis of compounds **B1, B2**. Reagents and conditions: (a). Amberlyst-15, MeOH, r.t., 40 min.

Reactions of **3a-3d, 3t** or **3w** with **4a** under the catalysis of CuO at 120 °C produced compounds **B3-B8** (Scheme 5).

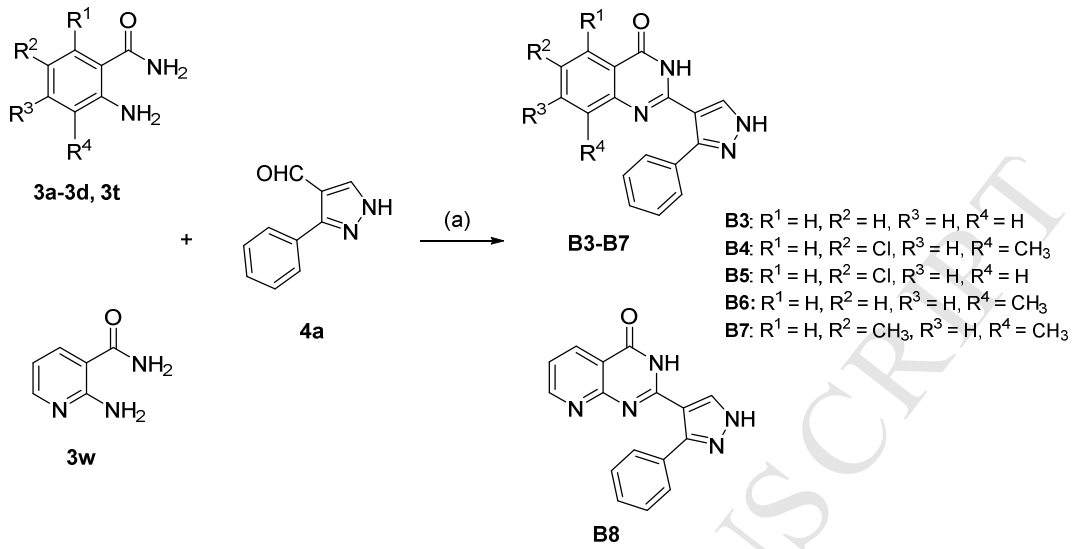

Scheme 5. Synthesis of compounds **B3-B8**. Reagents and conditions: (a). CuO, DMA, 120 °C, 24 h.

Treatment of substituted bromotoluene (**7a-7e**) with 1*H*-imidazole-4-carbaldehyde in the presence of anhydrous Na_2CO_3 and *tetra*-n-butylammonium iodide produced **8a-8e** [39], which were then reacted with **3a** using cyanuric chloride as catalyst to afford compounds **C1-C6** (Scheme 6).

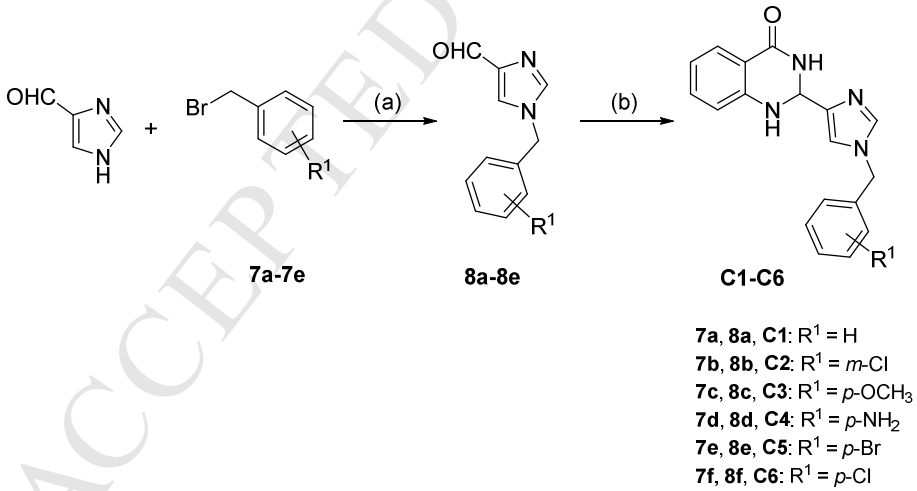

Scheme 6. Synthesis of compounds **C1-C6**. Reagents and conditions: (a). anhydrous Na_2CO_3, *tetra*-n-butylammonium iodide, THF, refluxed, 3 h; (b). **3a**, cyanuric chloride, DMSO, r.t., 0.5-2 h.

Commercially available 1-(4-chlorobenzyl)-1*H*-imidazole-5-carbaldehyde was reacted with **3a** in DMSO under the catalysis of cyanuric chloride to afford compound **C7** (Scheme 7).

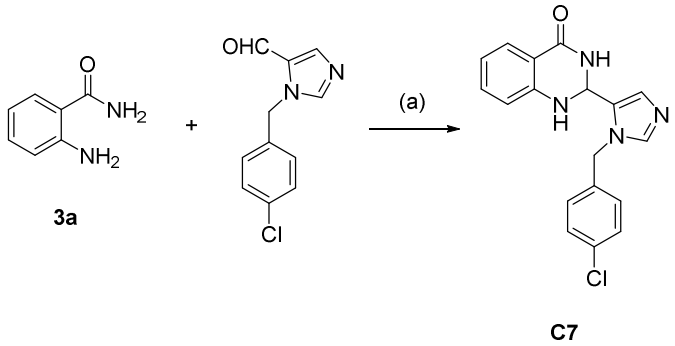

Scheme 7. Synthesis of compound **C7**. Reagents and conditions: (a). cyanuric chloride, DMSO, r.t., 2 h.

Pyrrole-2-carbaldehyde was reacted with N-bromosuccinimide in THF to give 4-bromo-1*H*-pyrrole-2-carbaldehyde, which was converted to 4-phenyl-1*H*-pyrrole-2-carbaldehyde (**9**) through Suzuki coupling reaction with phenylboronic acid under the catalytic system of $Pd(PPh_3)_4$ [40]. Subsequently, compound **C8** was prepared from **3a** and **9** through cyclocondensation reaction under the catalysis of cyanuric chloride (Scheme 8).

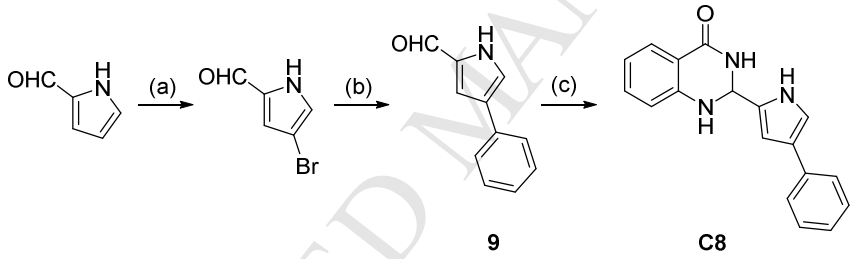

Scheme 8. Synthesis of compound **C8**. Reagents and conditions: (a). N-bromosuccinimide, THF, 0 °C, 15 min; (b). phenylboronic acid, $Pd(PPh_3)_4$, K_2CO_3, dioxane, water, 105 °C, 24 h; (c). **3a**, cyanuric chloride, DMSO, r.t., 2 h.

Methyl aryl ketones (**10b-10h)** were reacted with semicarbazide hydrochloride and anhydrous CH_3COONa in ethanol to afford semicarbazones (**11b-11h)**, which were then formylated by reacting with $POCl_3$-DMF complex to form 3-arylpyrazole-4-carboxaldehydes (**4b-4h)** [41]. Compounds **D1-D12** were obtained from **3a**, **3b**, **3k** or **3s** and **4b-4h** through cyclocondensation reaction in the presence of cyanuric chloride (Scheme 9).

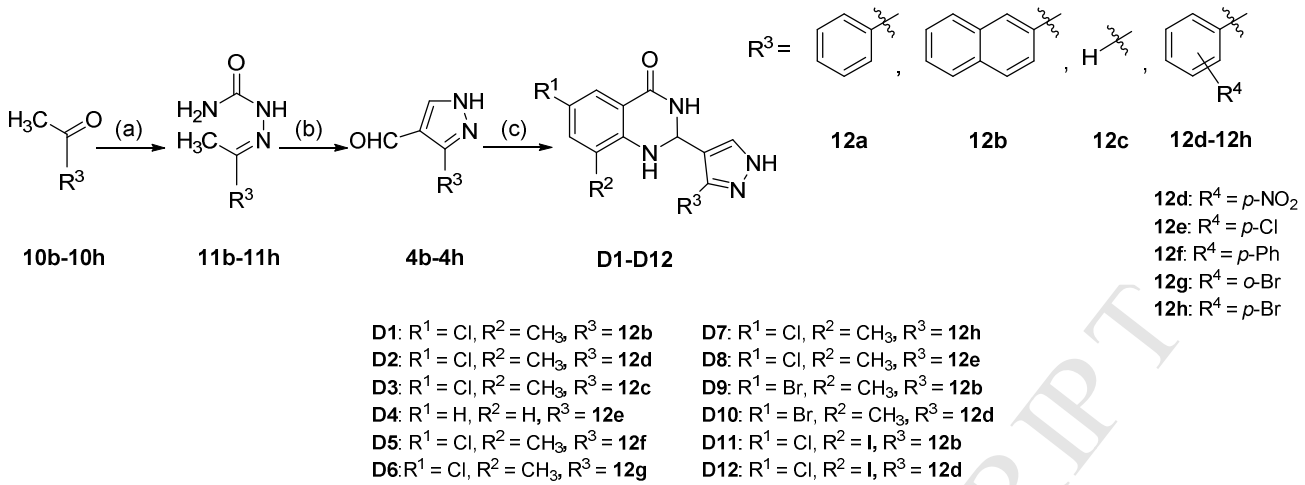

Scheme 9. Synthesis of compounds **D1-D12**. Reagents and conditions: (a). semicarbazide hydrochloride, anhydrous CH_3COONa, EtOH, reflux, 45 min, then methyl aryl ketone, reflux, 1 h, then r.t., 10 h; (b). $POCl_3$, DMF, 0 °C, 1 h, then semicarbazone, 80 °C, 1.5 h; (c). **3a**, **3b**, **3k** or **3s**, cyanuric chloride, MeOH or DMSO, r.t., 2 h.

2.3. Inhibitory activity and SAR

Totally, 53 compounds were synthesized and their biological activities were investigated. Fluorescent calcium imaging was used to evaluate their inhibitory activities preliminarily, and 33 of them obviously reduced H_2O_2-induced Ca^{2+} fluorescence increase (Fig. 3). Of them, 23 compounds reduced more than 50% Ca^{2+} fluorescence increase compared with the vehicle-treated cells. Their inhibitory activities against TRPM2 were then validated using whole-cell patch-clamp recordings (Table 1). At the concentration of 30 μM, 9 compounds inhibited about 90% TRPM2 currents. Their inhibitory activities at 3 μM were further tested. The concentration-dependent response curves of compounds that blocked more than half of the TRPM2 current at the concentration of 3 μM were plotted to calculate IC_{50} values. Four compounds, i.e. **A1**, **A10**, **D1** and **D9**, gave IC_{50} values of 3.7-5.1 μM (Fig. 4, Fig. S6). The TRPM2 nonspecific inhibitor ACA was used as a positive control.

As shown in Fig. 3 and Table 1, when the benzene ring of 2,3-dihydroquinazolin-4(1*H*)-one was replaced with pyridine, imidazole and thiazole (**A22-A25**), no inhibitory activity was observed for the resulting compounds. The introduction of alkyl, nitryl or halogen substituent (Me, NO_2, F, Cl, or Br) into the 5-, 6-, 7- and 8-positions of the 2,3-dihydroquinazolin-4(1*H*)-one (**A2**, **A4**-**A7**, **A17**, **A19** and **A21**) decreased the inhibitory activity compared with **H1**. However, a strong inhibitory activity (IC_{50} = 5.1 μM) was observed for 6, 8-position disubstituted 2,3-dihydroquinazolin-4(1*H*)-one derivative (**A1**) (6-chloro -8-methyl) (Fig. 4). To further investigate

the SAR of 6- and 8-position disubstituted 2,3-dihydroquinazolin-4(1*H*)-one derivatives, these positions were substituted with different groups (**A3**, **A8-A16**, **A18**, **A20**). We found compound **A10** (6-bromo-8-methyl) and **A18** (6-chloro-8-iodo) maintained the inhibitory activity, particularly **A10** showed an IC_{50} value of 4.6 μM (Fig. S6). But the other derivatives exhibited less potency than **H1**. These results indicated that introduction of a chlorine or bromine atom at 6-position accompanied by the presence of an iodine or methyl at 8-position were favorable for improving potency.

By replacing the carbonyl group at 4-position of the 2,3-dihydroquinazolin-4(1*H*)-one with sulfonyl group, compounds **B1** and **B2** were formed but no inhibitory activity was observed. Meanwhile, the introduction of carbon-carbon double bonds at the 1- and 2-position of the 2,3-dihydroquinazolin-4(1*H*)-one was investigated (**B3**-**B8**). It was found that the inhibitory activities were decreased. These results implied that the scaffold of 2,3-dihydroquinazolin-4(1*H*)-one is crucial for the inhibitory activity against TRPM2.

Replacing pyrazole ring at 2-position of the 2,3-dihydroquinazolin-4(1*H*)-one with imidazole ring along with the presence of substituted benzyl group at 1'-position of imidazole ring (**C1**-**C6**) also resulted in no inhibitory activity. To maintain the relative position of ring A and B (2,3-dihydroquinazolin-4(1*H*)-one) and ring D (substituted benzyl group), compound **C7** with substituted benzyl group at 5'-position of imidazole ring was synthesized, and a decreased inhibitory activity was observed. Compound **C8** with a pyrrole ring exhibited less potency than the pyrazole ring compound (**H1**), suggesting the importance of pyrazole ring for the inhibitory activity.

To further study the SAR of pyrazole ring derivatives, various substituted derivatives at 3'-position of the pyrazole ring were investigated (**D1**-**D8**). We found that: i) Removing the phenyl group at 3'-position of pyrazole ring (**D3**) exhibited lower inhibitory activity than **A1**. ii) Replacing the phenyl group at 3'-position of pyrazole ring with naphthyl group (**D1**) retained the inhibitory activity (IC_{50} = 4.0 μM) (Fig. S6). iii) A *p*-bromophenyl substituent at 3'-position of pyrazole ring (**D7**) displayed higher potency than the corresponding *o*-bromophenyl substituent (**D6**), which indicated that compounds containing *p*-substituted phenyl group could exhibit improved inhibitory activity. And compound **D2** (*p*-nitrophenyl) showed improved inhibitory activity compared with **D7.** These results demonstrated that the introduction of naphthyl or *p*-nitrophenyl substituent at 3'-position of pyrazole ring retained the inhibitory activity.

The 6, 8-position disubstituted 2,3-dihydroquinazolin-4(1*H*)-one (6-bromine-8-methyl and

6-chlorine-8-iodine) and the 3'-position substituted pyrazole ring (naphthyl and *p*-nitrophenyl) were combined (**D9**-**D12**) to generate more active inhibitors, and compound **D9** expectedly exhibited strong inhibitory activity with an IC_{50} = 3.7 μM (Fig. S6). Subsequently, we tested the inhibitory effect of **D9** in the D964A and H995A mutant channels. It exhibited less potency in the D964A mutant TRPM2 channel compared with the WT, and no inhibitory activity was observed in the H995A mutant TRPM2 channel (Fig. S7). These results suggested that both D964A and H995A were critically involved in the inhibition by extracellular **D9**.

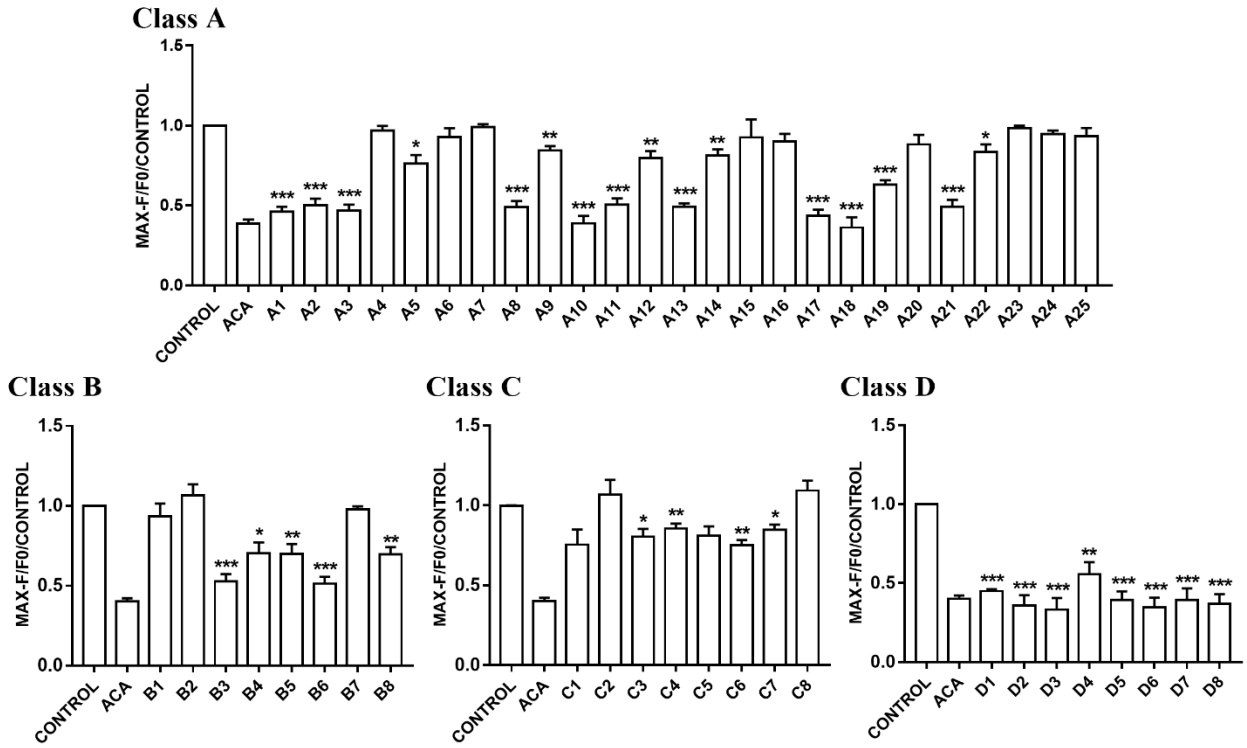

Fig. 3. Inhibition activity of compounds **A1-A25, B1-B8, C1-C8** and **D1-D8** against the TRPM2 channel preliminarily evaluated through calcium imaging method. Data were presented as mean ± SEM from at least three independent experiments, and ***$P < 0.005$, **$P < 0.01$, *$P < 0.05$.

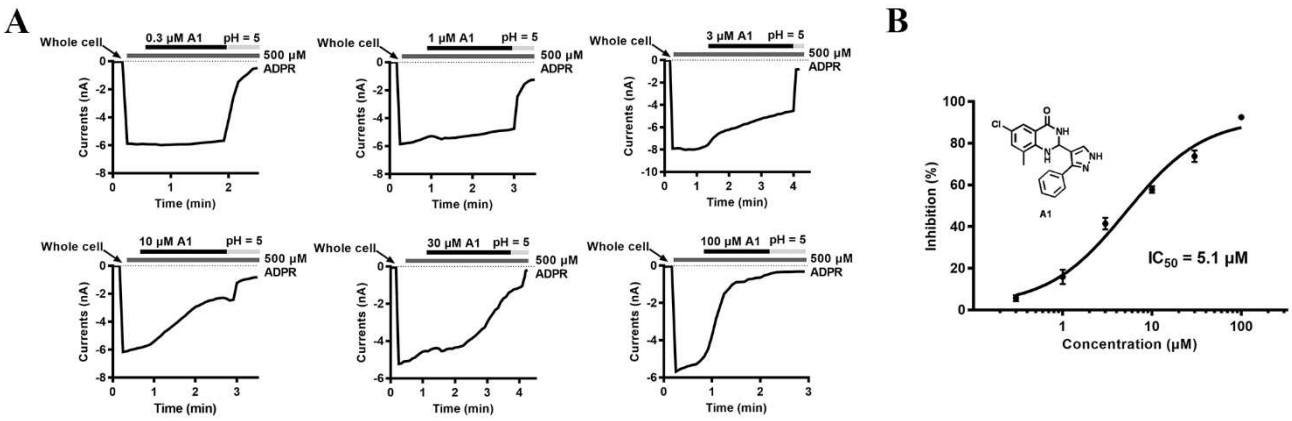

Fig. 4. Inhibition of the TRPM2 currents by **A1** in whole-cell patch-clamp recordings. (A) Representative currents of 500 μM ADPR-induced TRPM2 with extracellular treatment of compound **A1** at different concentrations. (B) Concentration-dependent inhibitory curve of compound **A1**. Data were presented as mean ± SEM from six independent experiments (n = 6).

Table 1

Inhibition activity of selected compounds against TRPM2 currents validated by whole-cell patch-clamping

compds	30 μM Inhibition (%)	3 μM Inhibition (%)	IC_{50} (μM)
H1	68.1±1.9%	--	--
A1	90.2±2.4%	46.4±2.8%	5.1
A2	27.9±2.2%	--	--
A3	60.5±4.1%	--	--
A8	42.7±5.5%	--	--
A10	92.8±0.3%	50.1±2.5%	4.6
A11	50.4±4.5%	--	--
A13	37.2±7.0%	--	--
A17	39.2±1.4%	--	--
A18	89.4±3.9%	39.6±6.2%	--
A21	34.8±0.9%	--	--
B3	28.7±2.1%	--	--
B6	21.2±1.2%	--	--
D1	90.2±4.8%	50.9±1.8%	4.0

D2	90.4±1.5%	43.4±3.6%	--
D3	16.9±5.1%	--	--
D5	17.0±4.9%	--	--
D6	17.9±4.0%	--	--
D7	51.0±7.2%	--	--
D8	10.3±2.9%	--	--
D9	--	48.7±5.1%	3.7
D10	--	42.1±3.7%	--
D11	--	19.9±4.8%	--
D12	--	34.9±7.1%	--
ACA	89.1±3.2%	75.9±6.8%	0.32

Percent inhibition at a test concentration are mean ± SEM from six determinations (n = 6).

"--" not determined.

2,3-Dihydroquinazolin-4(1*H*)-one derivatives possess a chiral center on C2 position. To study the influence of chirality on the TRPM2 inhibitor properties, we performed chiral separation on racemic **A1** using chiral high-performance liquid chromatography (HPLC) and obtained two enantiomers of **A1** (**A1-a**: $[\alpha]_D^{20}$ = -165.3 and **A1-b**: $[\alpha]_D^{20}$ = +164.0). We then characterized the absolute configuration of **A1-a** and **A1-b** by comparing experimental and calculated electronic circular dichroism (ECD) spectra [42]. As indicated in Fig. 5A, the calculated ECD spectrum of ***R*-A1** was similar to the experimental ECD spectrum of **A1-a**. Therefore, the absolute configuration of **A1-a** was confirmed to be ***R*-A1**. Similarly, the absolute configuration of **A1-b** was determined to be ***S*-A1**. Whole-cell patch-clamp recordings were performed on **A1**, ***R*-A1** and ***S*-A1**, respectively, at concentration of 30 μM. **A1**, ***R*-A1** and ***S*-A1** showed similar inhibitory activity against TRPM2 (Fig. 5B), suggesting the chirality had no influence on the inhibitory activity.

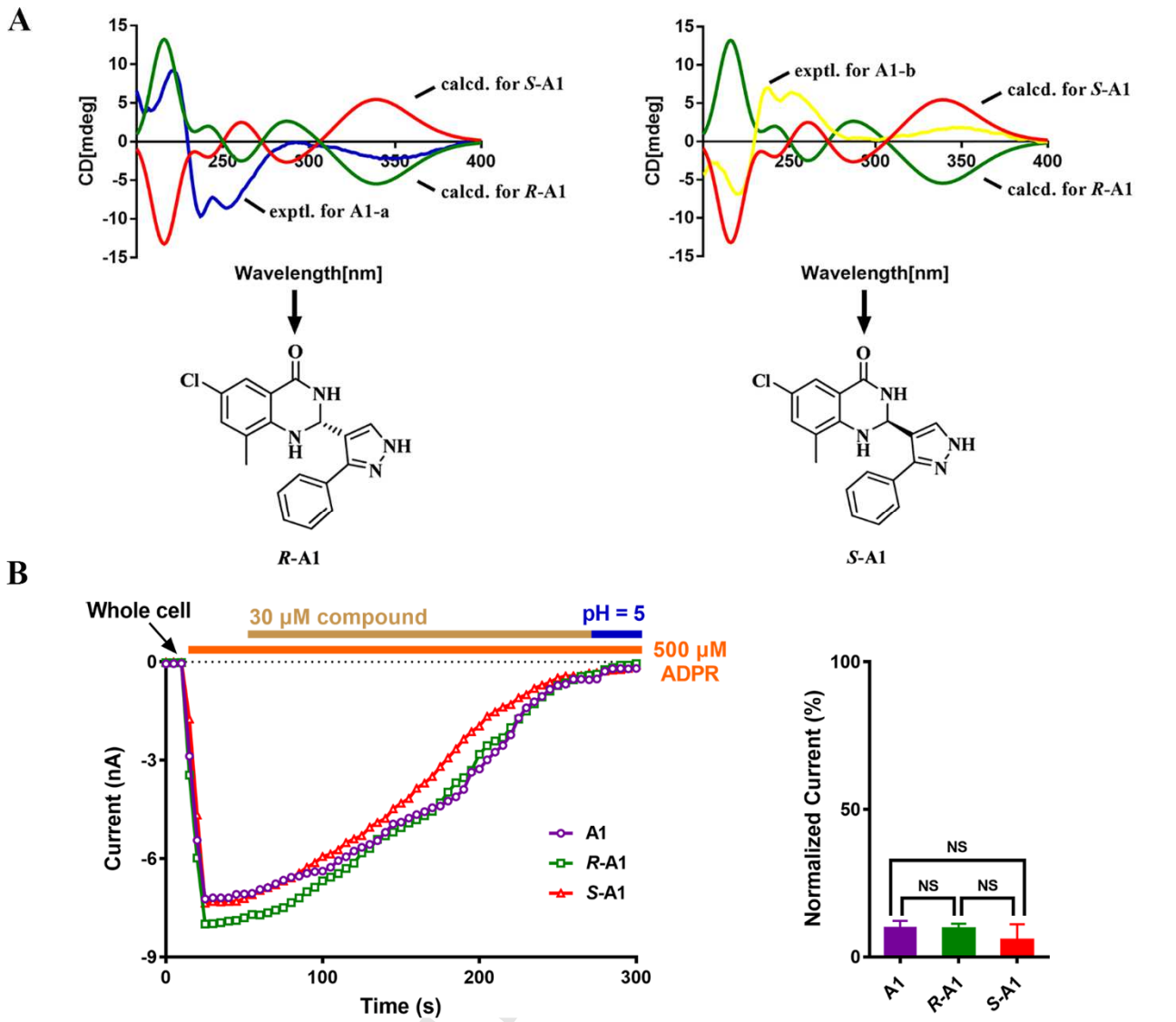

Fig. 5. Determination of the absolute configurations of two enantiomers of **A1** and inhibition of the TRPM2 currents by **A1**, ***R*-A1** and ***S*-A1** in whole-cell patch-clamp recordings. (A) Determination of the absolute configurations of two enantiomers of **A1** via a comparison of the calculated ECD spectra for ***R*-A1** and ***S*-A1** with the experimental ECD spectra for **A1-a** and **A1-b**. Calculated ECD spectra for ***R*-A1** at the B3LYP/6-31G* level in MeOH solution with the IEFPCM model (green line); calculated ECD spectra for ***S*-A1** at the B3LYP/6-31G* level in MeOH solution with the IEFPCM model (red line); experimental spectra for **A1-a** in MeOH (dark blue line); experimental spectra for **A1-b** in MeOH (yellow line). (B) Representative currents with extracellular treatments of 30 μM **A1** (purple), 30 μM ***R*-A1** (green) and 30 μM ***S*-A1** (red) showed similar inhibitory activity. Data were presented as mean ± SEM from six independent experiments (n = 6), and NS were presented as no significant difference for indicated comparisons.

Taken together, we found that naphthyl at 3'-position, methyl at 6-position and chlorine or bromine at 8-position of the 2,3-dihydroquinazolin-4(1*H*)-one were favorable for the inhibitory activity. Moreover, the chirality had no influence on inhibitory activity. Our investigation confirmed

that 2,3-dihydroquinazolin-4(1*H*)-one was a crucial scaffold, and the size and orientation of the substituents on the scaffold played key roles in the inhibitory activity against TRPM2.

*2.4. Inhibitory activity of Compounds **A1**, **A10**, **D1** and **D9** on the TRPM8 channel*

The TRPM8 channel is the closest related channel of TRPM2, and they share approximately 42% sequence identity [2]. The known non-nucleoside TRPM2 inhibitors such as 2-APB and ACA could also block the TRPM8 channel [22,43]. To evaluate the selectivity of **A1**, **A10**, **D1** and **D9**, the inhibitory activities of these compounds (30 μM) on the TRPM8 channel were tested by whole-cell patch-clamp recordings. TRPM8 currents overexpressed in HEK293 cells were activated by menthol and blocked by 2-APB.

As shown in Fig. 6, compared with the control, extracellular addition of **D1** and **D9** showed no significant effect on the TRPM8 currents, while **A1** and **A10** resulted in a mild reduction of TRPM8 current by 27% and 19%, respectively. The intracellular effects of these compounds were also tested, in which their applications in pipette exhibited similar effects to that of the extracellular treatments (Fig. S8). It is noteworthy that both **D1** and **D9** had a naphthyl group at the 3'-position of pyrazole ring, while **A1** and **A10** each had a phenyl group at this position, suggesting that the bulky naphthyl group was unfavorable for the inhibition of TRPM8 channel, and the substitute group at 3'-position of pyrazole ring played critical roles in the selectivity between the TRPM2 and TRPM8 channels.

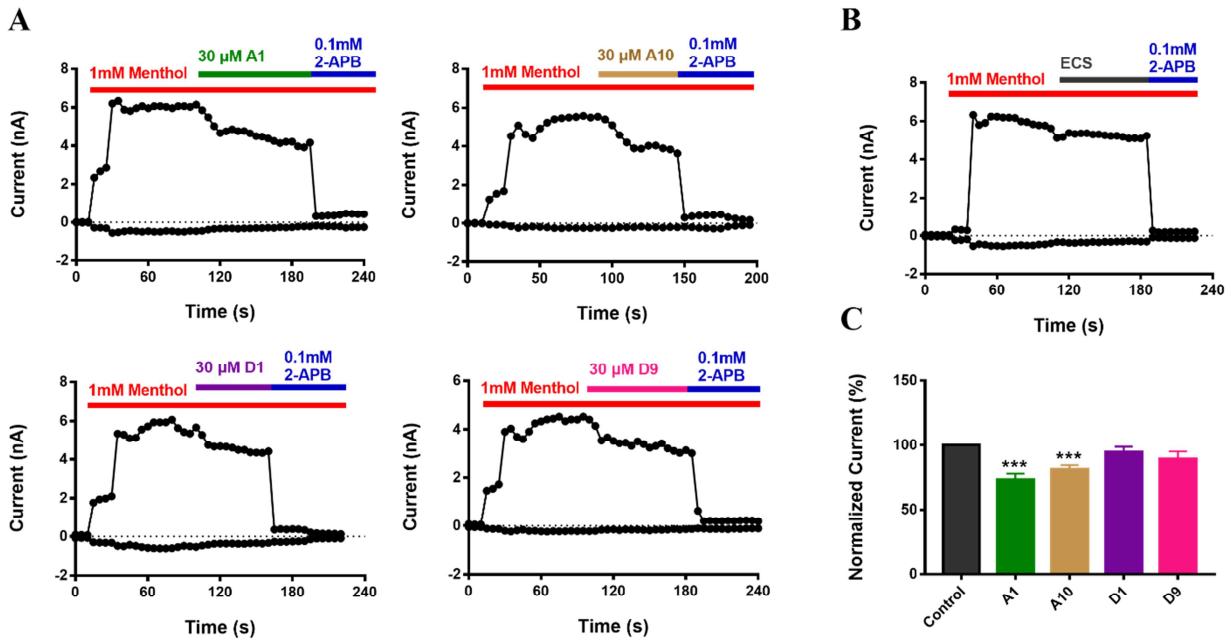

Fig. 6. Selectivity evaluations of extracellular 30 μM **A1, A10, D1** and **D9** on the TRPM8 channel. (A) Representative currents with extracellular treatments of 30 μM compounds. (B) The effect of control with its agonist (1 mM menthol) and inhibitor (0.1 mM 2-APB) on the TRPM8 channel (n = 5). (C) Mean peak currents

from recordings of (A) and (B), data were presented as mean ± SEM from five independent experiments (n = 5), and ***$P < 0.005$.

3. Conclusion

In this study, we discovered a potent TRPM2 inhibitor 2,3-dihydroquinazolin-4(1*H*)-one derivative **H1** by 3D similarity-based virtual screening. Fifty-three **H1** derivatives were designed and synthesized. Some of them exhibited strong inhibitory activity against the TRPM2 currents, especially compound **D9** with an IC_{50} value of 3.7 μM. More importantly, this compound showed specificity to the TRPM2 channel without affecting the TRPM8 current. In addition, the summarized SAR provided insights for the further development of specific TRPM2 inhibitors.

4. Experimental section

4.1. Materials and methods

All of chemicals and solvents used were obtained from commercial sources. The solvents were dried by standard procedures. Thin layer chromatography (Silica gel GF254, Qingdao Haiyang Chemical Co., Ltd, Qingdao, China) was employed to monitor reaction process, and silica column chromatography was carried out to purify crude product (Silica gel 200–300 mesh, Shanghai Sanpont Co., Ltd, Shanghai, China). ^{1}H NMR spectra and ^{13}C NMR spectra were recorded at 400 MHz using Bruker Avance III spectrometer (Bruker CO., Switzerland) in $CDCl_3$ or DMSO-d_6 solution with tetramethylsilane as internal standard and chemical shift values were given in ppm. The NMR data was processed by software MestReNova (Ver.6.1.0, mestrelab research S.L.). The splitting peak was designed as s, singlet; d, doublet; dd, double doublet; t, triplet; m, multiplet; br, broad. The high resolution mass (HRMS) was measured on FT-MS-Bruker APEX IV mass spectrometer.

4.2. Chemical synthesis

*4.2.1. General procedure for the synthesis of compounds **3a–3x***

The syntheses of compounds **3a-3x** were mainly referred to literature method [35].

A mixture of **1a-1q, 1w, 1x** (2 mmol), EDC•HCl (575 mg, 3 mmol), HOBt (446 mg, 3.3 mmol), NH_4Cl (348 mg, 6.5 mmol) and DIPEA (2.3 mL, 13 mmol) in DMSO (7 mL) was stirred at room temperature for 15 h. The mixture was extracted with EtOAc three times, and the combined organic layers were washed with brine, dried over anhydrous Na_2SO_4, filtered and concentrated under

reduced pressure to afford **3a-3q, 3w, 3x**.

A mixture of **2r-2v** (2 mmol) and NH_3•H_2O (25-28 wt%, 80 mmol) in sealed tube was heated at 100 °C for 12 h. The mixture was cooled to room temperature and extracted with EtOAc three times. The combined organic layers were washed with brine, dried over anhydrous Na_2SO_4, filtered and concentrated under reduced pressure to afford **3r-3v**.

*4.2.2. General procedure for the synthesis of compounds **4a–4h***

The syntheses of compounds **4a-4h** were mainly referred to literature method [41].

A mixture of semicarbazide hydrochloride (2 g, 17.9 mmol) and anhydrous CH_3COONa (2 g, 24.4 mmol) in EtOH (20 mL) was refluxed for 45 min and filtered while hot. **10a-10h** (16.6 mmol) was added to the filtrate, and the mixture was refluxed for 1 h. The mixture was stirred at room temperature for an additional 10 h, and the precipitate that formed was filtered and dried to afford **11a-11h**.

$POCl_3$ (3.6 mL, 39 mmol) was added dropwise to dry DMF (8.4 mL, 108 mmol) in ice bath, and the mixture was stirred at 0 °C for 1 h, followed by the addition of **11a-11h** (17 mmol) in small portions. The mixture was heated at 80 °C for 1.5 h and quickly poured onto ice (100 mL), then treated with 30% aqueous NaOH to adjust pH = 8-9, stirred for 30 min and neutralized with conc. HCl. After stirred at room temperature for additional 18 h, the resulting precipitate was filtered, washed with water, recrystallized from water and dried to afford **4a-4h**.

*4.2.3. General procedure for the synthesis of compounds **H1**, **A1–A23***

Cyanuric chloride (0.15 mmol) was added to a mixture of **3a-3x** (1 mmol) and **4a** (206 mg, 1.2 mmol) in CH_3CN, MeOH or DMSO (3 mL). The mixture was stirred at room temperature for 0.5-2 h. After completion, the mixture was extracted with EtOAc three times. The combined organic layers were washed with brine, dried over anhydrous Na_2SO_4, filtered and concentrated under reduced pressure. The crude product was purified by silica gel column chromatography eluting with CH_2Cl_2/MeOH (30/1) to afford **H1, A1-A23.**

4.2.3.1.

*2-(3-Phenyl-1H-pyrazol-4-yl)-2,3-dihydroquinazolin-4(1H)-one (**H1**)*

CH_3CN was employed as the solvent. Off-white solid. Yield: 66%. Mp 149–151 °C. ^{1}H NMR (400 MHz, DMSO-d_6) δ 13.24 (s, 0.5H), 13.09 (s, 0.5H), 8.16 (s, 1H), 8.04 (s, 0.5H), 7.75 (s, 0.5H), 7.71–7.59 (m, 3H), 7.53–7.32 (m, 3H), 7.26 (t, J = 7.6 Hz, 1H), 6.93 (s, 1H), 6.76–6.71 (m, 2H), 5.79 (d, J = 17.3 Hz, 1H). ^{13}C NMR (101 MHz, DMSO-d_6) δ 164.6, 149.1, 133.6, 130.4, 129.3, 128.8,

128.6, 128.0, 118.0, 116.1, 115.1, 60.7. HRMS (ESI–TOF$^+$) calcd for $C_{17}H_{15}N_4O$ $[M+H]^+$ *m/z* 291.1240, found 291.1242.

4.2.3.2.

*6-Chloro-8-methyl-2-(3-phenyl-1H-pyrazol-4-yl)-2,3-dihydroquinazolin-4(1H)-one (**A1**)*

MeOH was employed as the solvent. Off-white solid. Yield: 54%. Mp 175–177 °C. ^{1}H NMR (400 MHz, DMSO-d_6) δ 13.17 (s, 0.5H), 13.01 (s, 0.5H), 8.31 (s, 1H), 7.94 (s, 0.5H), 7.68–7.58 (m, 2H), 7.50–7.48 (m, 1.5H), 7.37 (dt, *J* = 39.2, 7.1 Hz, 2H), 7.21 (d, *J* = 1.8 Hz, 1H), 6.26 (d, *J* = 29.6 Hz, 1H), 5.79 (d, *J* = 34.6 Hz, 1H), 2.05 (s, 3H). ^{13}C NMR (101 MHz, DMSO-d_6) δ 163.6, 145.7, 133.7, 129.0, 128.6, 126.6, 124.7, 121.6, 117.8, 117.4, 60.3, 17.1. HRMS (ESI–TOF$^+$) calcd for $C_{18}H_{16}N_4OCl$ $[M+H]^+$ *m/z* 339.1013, found 339.1012.

4.2.3.3.

*6-Chloro-2-(3-phenyl-1H-pyrazol-4-yl)-2,3-dihydroquinazolin-4(1H)-one (**A2**)*

CH_3CN was employed as the solvent. Off-white solid. Yield: 65%. Mp 149–151 °C. ^{1}H NMR (400 MHz, DMSO-d_6) δ 13.26 (s, 0.5H), 13.12 (s, 0.5H), 8.35 (s, 1H), 8.06 (s, 0.5H), 7.77 (s, 0.5H), 7.70–7.59 (m, 3H), 7.51–7.31 (m, 3H), 7.31 (dd, *J* = 8.7, 2.5 Hz, 1H), 7.16 (s, 1H), 6.79 (d, *J* = 8.7 Hz, 1H), 5.83 (d, *J* = 26.6 Hz, 1H). ^{13}C NMR (101 MHz, DMSO-d_6) δ 163.4, 147.8, 133.3, 129.3, 128.8, 128.6, 127.1, 121.7, 117.5, 117.1, 60.5. HRMS (ESI–TOF$^+$) calcd for $C_{17}H_{14}N_4OCl$ $[M+H]^+$ *m/z* 325.0856, found 325.0864.

4.2.3.4.

*6,8-Dimethyl-2-(3-phenyl-1H-pyrazol-4-yl)-2,3-dihydroquinazolin-4(1H)-one (**A3**)*

CH_3CN was employed as the solvent. Off-white solid. Yield: 51%. Mp 154–156 °C. ^{1}H NMR (400 MHz, DMSO-d_6) δ 13.20 (s, 0.5H), 13.05 (s, 0.5H), 8.16 (s, 1H), 7.79–7.70 (m, 3H), 7.43 (d, *J* = 26.5 Hz, 4H), 7.01 (s, 1H), 5.83 (d, *J* = 44.3 Hz, 2H), 2.20 (s, 3H), 2.05 (s, 3H). ^{13}C NMR (101 MHz, DMSO-d_6) δ 165.0, 144.7, 135.4, 129.0, 128.5, 126.8, 125.7, 123.9, 118.2, 116.7, 60.5, 20.6, 17.2. HRMS (ESI–TOF$^+$) calcd for $C_{19}H_{19}N_4O$ $[M+H]^+$ *m/z* 319.1559, found 319.1559.

4.2.3.5.

*5-Chloro-2-(3-phenyl-1H-pyrazol-4-yl)-2,3-dihydroquinazolin-4(1H)-one (**A4**)*

CH_3CN was employed as the solvent. Off-white solid. Yield: 57%. Mp >320 °C. ^{1}H NMR (400 MHz, DMSO-d_6) δ 13.27 (s, 0.5H), 13.12 (s, 0.5H), 8.33 (s, 1H), 8.06 (s, 0.5H), 7.77 (s, 0.5H), 7.67 (d, *J* = 7.1 Hz, 1H), 7.59–7.50 (m, 2H), 7.45–7.33 (m, 2H), 7.24 (s, 1H), 7.19 (t, *J* = 7.9 Hz, 1H),

6.75 (d, *J* = 7.1 Hz, 2H), 5.66 (d, *J* = 14.9 Hz, 1H). ^{13}C NMR (101 MHz, DMSO-d_6) δ 162.1, 152.0, 134.4, 133.3, 128.9, 128.5, 121.1, 116.6, 114.6, 113.3, 59.8. HRMS (ESI–TOF$^+$) calcd for $C_{17}H_{14}N_4OCl$ $[M+H]^+$ *m/z* 325.0856, found 325.0855.

4.2.3.6.

*5-Methyl-2-(3-phenyl-1H-pyrazol-4-yl)-2,3-dihydroquinazolin-4(1H)-one (**A5**)*

CH_3CN was employed as the solvent. Off-white solid. Yield: 61%. Mp 269–271 °C. ^{1}H NMR (400 MHz, DMSO-d_6) δ 13.21 (s, 0.5H), 13.07 (s, 0.5H), 8.04–7.75 (m, 2H), 7.70–7.58 (m, 2H), 7.52–7.32 (m, 3H), 7.09 (t, *J* = 8.4 Hz, 1H), 6.80 (s, 1H), 6.65–6.52 (m, 2H), 5.63 (d, *J* = 24.5 Hz, 1H), 2.51 (s, 3H). ^{13}C NMR (101 MHz, DMSO-d_6) δ 165.2, 150.6, 140.9, 132.3, 128.8, 128.6, 121.8, 117.4, 114.7, 113.6, 60.2, 22.4. HRMS (ESI–TOF$^+$) calcd for $C_{18}H_{17}N_4O$ $[M+H]^+$ *m/z* 305.1402, found 305.1402.

4.2.3.7.

*8-Bromo-2-(3-phenyl-1H-pyrazol-4-yl)-2,3-dihydroquinazolin-4(1H)-one (**A6**)*

CH_3CN was employed as the solvent. Off-white solid. Yield: 53%. Mp 238–240 °C. ^{1}H NMR (400 MHz, DMSO-d_6) δ 13.20 (s, 0.5H), 13.05 (s, 0.5H), 8.51 (s, 1H), 7.88–7.60 (m, 5H), 7.47–7.41 (m, 3H), 6.74 (t, *J* = 7.5 Hz, 1H), 6.16–5.95 (m, 2H). ^{13}C NMR (101 MHz, DMSO-d_6) δ 163.2, 145.4, 136.8, 129.1, 128.6, 127.7, 119.5, 118.4, 118.2, 108.9, 60.1. HRMS (ESI– TOF$^+$) calcd for $C_{17}H_{14}N_4OBr$ $[M+H]^+$ *m/z* 369.0351, found 369.0352.

4.2.3.8.

*8-Nitro-2-(3-phenyl-1H-pyrazol-4-yl)-2,3-dihydroquinazolin-4(1H)-one (**A7**)*

DMSO was employed as the solvent. Yellow solid. Yield: 58%. Mp 248–250 °C. ^{1}H NMR (400 MHz, DMSO-d_6) δ 13.26 (s, 0.5H), 13.10 (s, 0.5H), 8.86 (s, 1H), 8.23–8.09 (m, 3H), 7.95–7.64 (m, 2H), 7.59–7.36 (m, 4H), 6.89 (t, *J* = 7.9 Hz, 1H), 6.18 (d, *J* = 43.9 Hz, 1H). ^{13}C NMR (101 MHz, DMSO-d_6) δ 161.9, 143.5, 135.8, 132.9, 130.7, 129.0, 128.5, 119.4, 118.2, 117.0, 59.7. HRMS (ESI–TOF$^+$) calcd for $C_{17}H_{14}N_5O_3$ $[M+H]^+$ *m/z* 336.1097, found 336.1101.

4.2.3.9.

*6-Fluoro-8-methyl-2-(3-phenyl-1H-pyrazol-4-yl)-2,3-dihydroquinazolin-4(1H)-one (**A8**)*

DMSO was employed as the solvent. Off-white solid. Yield: 56%. Mp 263–265 °C. ^{1}H NMR (400 MHz, DMSO-d_6) δ 13.22 (s, 0.5H), 13.05 (s, 0.5H), 8.38 (s, 1H), 7.98–7.61 (m, 3H), 7.50–7.35 (m, 3H), 7.26 (dd, *J* = 8.9, 3.0 Hz, 1H), 7.12–7.09 (m, 1H), 6.04 (d, *J* = 23.1 Hz, 1H), 5.78

(d, J = 11.3 Hz, 1H), 2.10 (s, 3H). ^{13}C NMR (101 MHz, DMSO-d_6) δ 164.0, 155.3 (d, J_{CF} = 235.3 Hz), 143.5, 139.8, 128.9, 128.5, 127.0, 121.6 (d, J_{CF} = 23.2 Hz), 117.9, 110.6 (d, J_{CF} = 23.2 Hz), 60.5, 17.3. ^{19}F NMR (376 MHz, DMSO-d_6) δ -126.03 (d, J = 94.0 Hz). HRMS (ESI–TOF$^+$) calcd for $C_{18}H_{16}N_4OF$ $[M+H]^+$ *m/z* 323.1308, found 323.1304.

4.2.3.10.

*6, 8-Dichloro-2-(3-phenyl-1H-pyrazol-4-yl)-2,3-dihydroquinazolin-4(1H)-one (**A9**)*

DMSO was employed as the solvent. Off-white solid. Yield: 61%. Mp 149–151 °C. ^{1}H NMR (400 MHz, DMSO-d_6) δ 13.20 (s, 0.5H), 13.04 (s, 0.5H), 8.62 (d, J = 7.7 Hz, 1H), 7.92–7.67 (m, 2H), 7.61 (d, J = 10.9 Hz, 3H), 7.52–7.34 (m, 3H), 6.71 (dd, J = 46.5, 8.1 Hz, 1H), 5.93 (dd, J = 33.1, 7.3 Hz, 1H). ^{13}C NMR (101 MHz, DMSO-d_6) δ 162.1, 143.5, 132.8, 130.1, 129.2, 128.8, 128.7, 128.0, 126.4, 118.1, 60.1. HRMS (ESI–TOF$^+$) calcd for $C_{17}H_{13}N_4OCl_2$ $[M+H]^+$ *m/z* 359.0466, found 359.0464.

4.2.3.11.

*6-Bromo-8-methyl-2-(3-phenyl-1H-pyrazol-4-yl)-2,3-dihydroquinazolin-4(1H)-one (**A10**)*

DMSO was employed as the solvent. Off-white solid. Yield: 66%. Mp 153–155 °C. ^{1}H NMR (400 MHz, DMSO-d_6) δ 8.37 (s, 1H), 7.86–7.63 (m, 4H), 7.48–7.34 (m, 4H), 6.34 (s, 1H), 5.82 (s, 1H), 2.08 (s, 3H). ^{13}C NMR (101 MHz, DMSO-d_6) δ 163.5, 146.1, 136.3, 129.0, 128.6, 127.7, 126.9, 117.9, 117.8, 109.1, 60.2, 17.1. HRMS (ESI–TOF$^+$) calcd for $C_{18}H_{16}N_4OBr$ $[M+H]^+$ *m/z* 383.0507, found 383.0497.

4.2.3.12.

*6-Bromo-8-methoxy-2-(3-phenyl-1H-pyrazol-4-yl)-2,3-dihydroquinazolin-4(1H)-one (**A11**)*

DMSO was employed as the solvent. Off-white solid. Yield: 59%. Mp 243–245 °C. ^{1}H NMR (400 MHz, DMSO-d_6) δ 13.16 (s, 0.5H), 13.01 (s, 0.5H), 8.34 (s, 1H), 7.81 (dd, J = 57.9, 5.3 Hz, 1H), 7.64 (s, 2H), 7.45–7.36 (m, 4H), 7.12 (d, J = 2.1 Hz, 1H), 6.25 (s, 1H), 5.84 (s, 1H), 3.77 (s, 3H). ^{13}C NMR (101 MHz, DMSO-d_6) δ 163.0, 148.0, 138.2, 129.0, 128.7, 121.5, 118.0, 117.1, 116.7, 108.7, 60.5, 56.6. HRMS (ESI–TOF$^+$) calcd for $C_{18}H_{16}N_4O_2Br$ $[M+H]^+$ *m/z* 399.0388, found 399.0388.

4.2.3.13.

*8-Bromo-6-methyl-2-(3-phenyl-1H-pyrazol-4-yl)-2,3-dihydroquinazolin-4(1H)-one (**A12**)*

DMSO was employed as the solvent. Off-white solid. Yield: 47%. Mp 141–143 °C. ^{1}H NMR (400 MHz, DMSO-d_6) δ 13.19 (s, 0.5H), 13.01 (s, 0.5H), 8.45 (d, J = 10.9 Hz, 1H), 7.87–7.61 (m, 3H), 7.54–7.34 (m, 5H), 5.94 (d, J = 12.8 Hz, 1H), 5.83 (d, J = 5.1 Hz, 1H), 2.23 (s, 3H). ^{13}C NMR (101 MHz, DMSO-d_6) δ 163.4, 143.2, 137.1, 129.9, 129.2, 128.9, 128.5, 127.9, 118.3, 109.0, 60.3, 20.1. HRMS (ESI–TOF^{+}) calcd for $C_{18}H_{16}N_4OBr$ $[M+H]^+$ *m/z* 383.0507, found 383.0498.

4.2.3.14.

*6, 8-Difluoro-2-(3-phenyl-1H-pyrazol-4-yl)-2,3-dihydroquinazolin-4(1H)-one (**A13**)*

DMSO was employed as the solvent. Off-white solid. Yield: 45%. Mp 237–239 °C. ^{1}H NMR (400 MHz, DMSO-d_6) δ 13.21 (s, 0.5H), 13.07 (s, 0.5H), 8.51 (d, J = 8.7 Hz, 1H), 8.01 (s, 0.5H), 7.72–7.69 (m, 1.5H), 7.61 (d, J = 7.3 Hz, 1H), 7.51 (t, J = 7.5 Hz, 1H), 7.45–7.33 (m, 3H), 7.28 (d, J = 8.6 Hz, 1H), 6.82 (d, J = 17.5 Hz, 1H), 5.83 (d, J = 26.6 Hz, 1H). ^{13}C NMR (101 MHz, DMSO-d_6) δ 162.5, 153.9 (dd, J_{CF} = 237.4, 11.1 Hz), 150.3 (dd, J_{CF} = 247.5, 10.1 Hz), 149.4, 134.1 (dd, J_{CF} = 14.1, 2.0 Hz), 129.2, 128.7, 118.7 (d, J_{CF} = 17.2 Hz), 117.4 (d, J_{CF} = 14.1 Hz), 109.0 (d, J_{CF} = 23.2 Hz), 108.6, 108.4 (d, J_{CF} = 6.1 Hz), 108.1, 60.6 (d, J_{CF} = 29.3 Hz). ^{19}F NMR (376 MHz, DMSO-d_6) δ -123.67 (d, J = 60.2 Hz), -128.46 (d, J = 48.9 Hz). HRMS (ESI–TOF^{+}) calcd for $C_{17}H_{13}N_4OF_2$ $[M+H]^+$ *m/z* 327.1057, found 327.1060.

4.2.3.15.

*8-Bromo-6-fluoro-2-(3-phenyl-1H-pyrazol-4-yl)-2,3-dihydroquinazolin-4(1H)-one (**A14**)*

DMSO was employed as the solvent. Off-white solid. Yield: 47%. Mp 256–258 °C. ^{1}H NMR (400 MHz, DMSO-d_6) δ 13.21 (s, 0.5H), 13.04 (s, 0.5H), 8.66 (d, J = 10.3 Hz, 1H), 7.90–7.61 (m, 4H), 7.53–7.34 (m, 4H), 6.10 (d, J = 53.0 Hz, 1H), 5.90 (d, J = 34.2 Hz, 1H). ^{13}C NMR (101 MHz, DMSO-d_6) δ 162.4, 154.8 (dd, J_{CF} = 239.4, 10.1 Hz), 149.0, 142.5 (d, J_{CF} = 12.1, Hz), 139.3, 134.1, 129.3, 128.9, 128.6, 128.0, 124.2 (d, J_{CF} = 26.3 Hz), 128.6 (dd, J_{CF} = 32.3, 6.1 Hz), 118.0 (d, J_{CF} = 11.1 Hz), 113.5 (d, J_{CF} = 23.2 Hz), 109.4 (dd, J_{CF} = 29.3, 9.1 Hz), 60.2 (d, J_{CF} = 28.3 Hz). ^{19}F NMR (376 MHz, DMSO-d_6) δ -123.83 (d, J = 127.8 Hz). HRMS (ESI–TOF^{+}) calcd for $C_{17}H_{13}N_4OFBr$ $[M+H]^+$ *m/z* 387.0257, found 387.0259.

4.2.3.16.

*6, 8-Diiodo-2-(3-phenyl-1H-pyrazol-4-yl)-2,3-dihydroquinazolin-4(1H)-one (**A15**)*

DMSO was employed as the solvent. Off-white solid. Yield: 53%. Mp 151–153 °C. ^{1}H NMR (400 MHz, DMSO-d_6) δ 13.23 (s, 0.5H), 13.03 (s, 0.5H), 8.61 (s, 1H), 8.04–7.58 (m, 5H), 7.43 (t, J

= 24.7 Hz, 3H), 5.98 (d, *J* = 38.3 Hz, 2H). ^{13}C NMR (101 MHz, DMSO-d_6) δ 162.1, 149.3, 147.5, 136.4, 134.0, 129.8, 129.3, 128.9, 128.5, 128.4, 128.1, 119.2, 119.0, 118.4, 87.0, 81.0, 60.0. HRMS (ESI–TOF$^+$) calcd for $C_{17}H_{13}N_4OI_2$ $[M+H]^+$ *m/z* 542.9179, found 542.9179.

4.2.3.17.

*6-Iodo-8-methyl-2-(3-phenyl-1H-pyrazol-4-yl)-2,3-dihydroquinazolin-4(1H)-one (**A16**)*

DMSO was employed as the solvent. Off-white solid. Yield: 61%. Mp 226–228 °C. ^{1}H NMR (400 MHz, DMSO-d_6) δ 13.22 (s, 0.5H), 13.06 (s, 0.5H), 8.33 (s, 1H), 7.98–7.61 (m, 4H), 7.50–7.36 (m, 4H), 6.34 (d, *J* = 19.2 Hz, 1H), 5.82 (d, *J* = 24.6 Hz, 1H), 2.05 (s, 3H). ^{13}C NMR (101 MHz, DMSO-d_6) δ 163.4, 146.5, 141.8, 133.9, 129.2, 128.8, 128.6, 128.0, 127.0, 128.0, 60.3, 16.9. HRMS (ESI–TOF$^+$) calcd for $C_{18}H_{16}N_4OI$ $[M+H]^+$ *m/z* 431.0369, found 431.0365.

4.2.3.18.

*8-Methyl-2-(3-phenyl-1H-pyrazol-4-yl)-2,3-dihydroquinazolin-4(1H)-one (**A17**)*

CH_3CN was employed as the solvent. Off-white solid. Yield: 63%. Mp 262–264 °C. ^{1}H NMR (400 MHz, DMSO-d_6) δ 13.20 (s, 0.5H), 13.04 (s, 0.5H), 8.20 (s, 1H), 7.96–7.55 (m, 4H), 7.50–7.37 (m, 3H), 7.16 (d, *J* = 6.4 Hz, 1H), 6.71–6.67 (m, 1H), 6.06 (d, *J* = 25.5 Hz, 1H), 5.79 (d, J = 27.7 Hz, 1H), 2.06 (s, 3H). ^{13}C NMR (101 MHz, DMSO-d_6) δ 164.8, 146.8, 134.4, 128.9, 128.6, 128.0, 125.8, 123.7, 118.0, 116.5, 60.4, 17.3. HRMS (ESI–TOF$^+$) calcd for $C_{18}H_{17}N_4O$ $[M+H]^+$ *m/z* 305.1402, found 305.1404.

4.2.3.19.

*6-Chloro-8-iodo-2-(3-phenyl-1H-pyrazol-4-yl)-2,3-dihydroquinazolin-4(1H)-one (**A18**)*

DMSO was employed as the solvent. Off-white solid. Yield: 50%. Mp 267–269 °C. ^{1}H NMR (400 MHz, DMSO-d_6) δ 13.23 (s, 0.5H), 13.03 (s, 0.5H), 8.66 (d, *J* = 6.8 Hz, 1H), 7.85–7.58 (m, 5H), 7.53–7.34 (m, 3H), 6.03–5.89 (m, 2H). ^{13}C NMR (101 MHz, DMSO-d_6) δ 162.3, 141.7, 129.3, 129.0, 128.5, 127.6, 123.3, 118.3, 118.0, 86.2, 60.2. HRMS (ESI–TOF$^+$) calcd for $C_{17}H_{13}N_4OClI$ $[M+H]^+$ *m/z* 450.9823, found 450.9823.

4.2.3.20.

*7-Bromo-2-(3-phenyl-1H-pyrazol-4-yl)-2,3-dihydroquinazolin-4(1H)-one (**A19**)*

CH_3CN was employed as the solvent. Off-white solid. Yield: 59%. Mp 238–240 °C. ^{1}H NMR (400 MHz, DMSO-d_6) δ 13.27 (s, 0.5H), 13.12 (s, 0.5H), 8.28 (s, 1H), 8.06 (s, 0.5H), 7.76 (s, 0.5H), 7.58–7.37 (m, 3H), 7.50–7.37 (m, 3H), 7.19 (s, 1H), 6.94 (s, 1H), 6.88 (dd, *J* = 8.3, 1.5 Hz, 1H), 5.85

(d, J = 23.3 Hz, 1H). ^{13}C NMR (101 MHz, DMSO-d_6) δ 163.8, 150.1, 130.1, 129.3, 128.8, 128.6, 127.1, 120.8, 117.1, 115.0, 60.6. HRMS (ESI–TOF$^+$) calcd for $C_{17}H_{14}N_4OBr$ $[M+H]^+$ *m/z* 369.0351, found 369.0352.

4.2.3.21.

*6, 8-Dibromo-2-(3-phenyl-1H-pyrazol-4-yl)-2,3-dihydroquinazolin-4(1H)-one (**A20**)*

DMSO was employed as the solvent. Off-white solid. Yield: 67%. Mp 156–158 °C. ^{1}H NMR (400 MHz, DMSO-d_6) δ 13.19 (s, 0.5H), 13.02 (s, 0.5H), 8.63–7.88 (m, 2H), 7.81–7.60 (m, 4H), 7.50–7.35 (m, 3H), 6.41 (d, J = 57.3 Hz, 1H), 5.93 (d, J = 36.0 Hz, 1H). ^{13}C NMR (101 MHz, DMSO-d_6) δ 162.0, 144.8, 138.2, 129.9, 128.9, 128.6, 119.1, 118.2, 109.9, 109.2, 60.1. HRMS (ESI–TOF$^+$) calcd for $C_{17}H_{13}N_4OBr_2$ $[M+H]^+$ *m/z* 446.9456, found 446.9450.

4.2.3.22.

*6-Fluoro-2-(3-phenyl-1H-pyrazol-4-yl)-2,3-dihydroquinazolin-4(1H)-one (**A21**)*

CH_3CN was employed as the solvent. Off-white solid. Yield: 62%. Mp 104–106 °C. ^{1}H NMR (400 MHz, DMSO-d_6) δ 13.25 (s, 0.5H), 13.10 (s, 0.5H), 8.35 (s, 1H), 8.05 (s, 0.5H), 7.77 (s, 0.5H), 7.70–7.59 (m, 2H), 7.53–7.34 (m, 4H), 7.20–7.15 (m, 1H), 6.92 (s, 1H), 6.81–6.77 (m, 1H), 5.78 (d, J = 26.1 Hz, 1H). ^{13}C NMR (101 MHz, DMSO-d_6) δ 163.7, 155.5 (d, J_{CF} = 235.3 Hz), 145.8, 128.8, 128.6, 121.0 (d, J_{CF} = 23.2 Hz), 117.4, 116.9, 116.8, 113.1 (d, J_{CF} = 22.2 Hz), 60.8. ^{19}F NMR (376 MHz, DMSO-d_6) δ -126.23. HRMS (ESI–TOF$^+$) calcd for $C_{17}H_{14}N_4OF$ $[M+H]^+$ *m/z* 309.1152, found 309.1152.

4.2.3.23.

*2-(3-Phenyl-1H-pyrazol-4-yl)-2,3-dihydropyrido[2,3-d]pyrimidin-4(1H)-one (**A22**)*

DMSO was employed as the solvent. Off-white solid. Yield: 48%. Mp 178–180 °C. ^{1}H NMR (400 MHz, DMSO-d_6) δ 13.20 (s, 0.5H), 13.09 (s, 0.5H), 8.36 (s, 1H), 8.16 (d, J = 4.1 Hz, 1H), 7.96–7.66 (m, 5H), 7.45–7.39 (m, 3H), 6.78–6.75 (m, 1H), 5.96 (s, 1H). ^{13}C NMR (101 MHz, DMSO-d_6) δ 163.7, 158.8, 153.1, 136.3, 128.9, 128.7, 118.0, 114.6, 110.4, 59.6. HRMS (ESI– TOF$^+$) calcd for $C_{16}H_{14}N_5O$ $[M+H]^+$ *m/z* 292.1198, found 292.1201.

4.2.3.24.

*2-(3-Phenyl-1H-pyrazol-4-yl)-2,3-dihydropyrido[3,4-d]pyrimidin-4(1H)-one (**A23**)*

DMSO was employed as the solvent. Yellow solid. Yield: 47%. Mp 200–202 °C. ^{1}H NMR (400 MHz, DMSO-d_6) δ 13.28 (s, 0.5H), 13.13 (s, 0.5H), 8.52 (s, 1H), 8.17 (s, 1H), 8.07 (s, 0.5H),

7.98 (d, J = 4.4 Hz, 1H), 7.77 (s, 0.5H), 7.70–7.59 (m, 2H), 7.53–7.35 (m, 4H), 7.23 (s, 1H), 5.89 (d, J = 26.8 Hz, 1H). ^{13}C NMR (101 MHz, DMSO-d_6) δ 163.1, 144.0, 139.1, 138.5, 129.3, 128.6, 120.9, 120.3, 117.3, 60.5. HRMS (ESI–TOF$^+$) calcd for $C_{16}H_{14}N_5O$ $[M+H]^+$ *m/z* 292.1198, found 292.1201.

*4.2.4. General procedure for the synthesis of compounds **A24, A25***

A mixture of **4a** (172 mg, 1 mmol), **5a** or **5b** (1 mmol) and 2-morpholinoethanesulfonic acid (20 mg, 0.1 mmol) in 50% aq EtOH (10 mL) was heated at 60 °C for 3 h, and the solvent was removed under reduced pressure. The residue was extracted with EtOAc three times, and the combined organic layers were washed with brine, dried over anhydrous Na_2SO_4, filtered and concentrated. The crude product was purified by silica gel column chromatography eluting with CH_2Cl_2/MeOH (30/1) to afford **A24** or **A25**, respectively.

4.2.4.1.

*2-(3-Phenyl-1H-pyrazol-4-yl)-2,3,4,9-tetrahydro-1H-purin-6(5H)-one (**A24**)*

Off-white solid. Yield: 43%. Mp 273–275 °C. ^{1}H NMR (400 MHz, DMSO-d_6) δ 13.57 (s, 1H), 12.80 (s, 1H), 9.15 (s, 1H), 8.43 (s, 1H), 7.69–7.63 (m, 4H), 7.55–7.44 (m, 4H). ^{13}C NMR (101 MHz, DMSO-d_6) δ 161.4, 151.6, 148.2, 136.2, 129.3, 129.0, 117.6, 117.2. HRMS (ESI–TOF$^+$) calcd for $C_{14}H_{13}N_6O$ $[M+H]^+$ *m/z* 281.1151, found 281.1158.

4.2.4.2.

*2-(3-Phenyl-1H-pyrazol-4-yl)-2,3-dihydrothieno[2,3-d]pyrimidin-4(1H)-one (**A25**)*

Yellow solid. Yield: 41%. Mp 245–247 °C. ^{1}H NMR (400 MHz, DMSO-d_6) δ 13.73 (s, 1H), 8.51–8.45 (m, 2H), 7.97 (s, 1H), 7.68 (d, J = 6.4 Hz, 2H), 7.57–7.50 (m, 3H), 7.32 (d, J = 8.9 Hz, 2H), 7.20 (d, J = 5.6 Hz, 1H). ^{13}C NMR (101 MHz, DMSO-d_6) δ 163.7, 155.6, 153.4, 129.4, 129.2, 129.1, 128.8, 119.4, 116.4. HRMS (ESI–TOF$^+$) calcd for $C_{15}H_{13}N_4OS$ $[M+H]^+$ *m/z* 297.0810, found 297.0811.

*4.2.5. General procedure for the synthesis of compounds **B1, B2***

A mixture of **4a** or **4e** (1.2 mmol), **6** (172 mg, 1 mmol) and Amberlyst-15 (10%, w/w) in MeOH (3 mL) underwent ultrasound irradiation (40 KHz) at room temperature for 40 min, and EtOAc was added to the reaction. The mixture was filtered, and the filtrate was washed with brine, dried over anhydrous Na_2SO_4, filtered and concentrated under reduced pressure. The crude product was purified by recrystallization from EtOAc:PE:MeOH = 3:2:1 to afford **B1** or **B2**, respectively.

4.2.5.1.

*3-(3-Phenyl-1H-pyrazol-4-yl)-3,4-dihydro-2H-benzo[e][1,2,4]thiadiazine 1,1-dioxide (**B1**)*

Off-white solid. Yield: 61%. Mp 226–228 °C. ^{1}H NMR (400 MHz, DMSO-d_6) δ 13.36 (s, 0.5H), 13.16 (s, 0.5H), 8.10–7.94 (m, 2H), 7.69–7.38 (m, 7H), 7.32 (t, J = 7.8 Hz, 1H), 6.90 (d, J = 6.3 Hz, 1H), 6.77 (t, J = 7.6 Hz, 1H), 5.79 (dd, J = 26.9, 10.2 Hz, 1H). ^{13}C NMR (101 MHz, DMSO-d_6) δ 144.2, 133.3, 129.2, 128.1, 124.2, 121.9, 117.2, 116.8, 115.4, 61.6. HRMS (ESI–TOF$^+$) calcd for $C_{16}H_{15}N_4O_2S$ $[M+H]^+$ *m/z* 327.0910, found 327.0916.

4.2.5.2.

*3-(3-(4-Chlorophenyl)-1H-pyrazol-4-yl)-3,4-dihydro-2H-benzo[e][1,2,4]thiadiazine 1,1-dioxide (**B2**)*

Off-white solid. Yield: 45%. Mp 254–256 °C. ^{1}H NMR (400 MHz, DMSO-d_6) δ 13.44, 13.24 (s, 1H), 8.10–7.95 (m, 2H), 7.71–7.48 (m, 6H), 7.33 (t, J = 7.8 Hz, 1H), 6.90 (d, J = 6.8 Hz, 1H), 6.77 (t, J = 6.4 Hz, 1H), 5.83–5.72 (m, 1H). ^{13}C NMR (101 MHz, DMSO-d_6) δ 147.6, 144.1, 133.3, 133.1, 132.5, 130.4, 129.8, 129.7, 129.2, 124.2, 121.9, 117.3, 116.9, 115.9, 115.5, 61.7. HRMS (ESI–TOF$^+$) calcd for $C_{16}H_{14}N_4O_2ClS$ $[M+H]^+$ *m/z* 361.0521, found 361.0529.

*4.2.6. General procedure for the synthesis of compounds **B3-B8***

A mixture of **3a-3d, 3t** or **3w** (1 mmol), **4a** (172 mg, 1 mmol) and CuO (4 mg, 0.05 mmol) in DMA (3 mL) was heated at 120 °C for 24 h. The mixture was cooled to room temperature and extracted with EtOAc three times. The combined organic layers were washed with brine, dried over anhydrous Na_2SO_4, filtered and concentrated under reduced pressure. The crude product was purified by silica gel column chromatography eluting with CH_2Cl_2/MeOH (30/1) to afford **B3-B8**.

4.2.6.1.

*2-(3-Phenyl-1H-pyrazol-4-yl)quinazolin-4(3H)-one (**B3**)*

Off-white solid. Yield: 50%. Mp 267–269 °C. ^{1}H NMR (400 MHz, DMSO-d_6) δ 13.59 (s, 0.5H), 13.41 (s, 0.5H), 12.22 (s, 1H), 8.46 (s, 0.5H), 8.19 (s, 0.5H), 8.12 (d, J = 7.6 Hz, 1H), 7.77–7.70 (m, 3H), 7.48–7.37 (m, 5H). ^{13}C NMR (101 MHz, DMSO-d_6) δ 162.5, 149.5, 149.2, 134.8, 129.3, 129.1, 128.6, 128.2, 127.4, 126.5, 126.2, 121.3, 113.4, 113.0. HRMS (ESI–TOF$^+$) calcd for $C_{17}H_{13}N_4O$ $[M+H]^+$ *m/z* 289.1089, found 289.1090.

4.2.6.2.

*6-Chloro-8-methyl-2-(3-phenyl-1H-pyrazol-4-yl)quinazolin-4(3H)-one (**B4**)*

Off-white solid. Yield: 44%. Mp 272–274 °C. ^{1}H NMR (400 MHz, DMSO-d_6) δ 13.59 (s, 0.5H), 13.41 (s, 0.5H), 12.37 (s, 1H), 8.55 (s, 0.5H), 8.30 (s, 0.5H), 7.86 (d, J = 3.6 Hz, 1H), 7.68–7.62 (m, 3H), 7.41 (d, J = 36.9 Hz, 3H), 2.10 (s, 3H). ^{13}C NMR (101 MHz, DMSO-d_6) δ 161.9,

148.2, 146.8, 138.7, 134.7, 129.9, 129.6, 128.2, 122.6, 122.1, 113.1, 17.1. HRMS (ESI–TOF$^+$) calcd for $C_{18}H_{14}N_4OCl$ $[M+H]^+$ *m/z* 337.0856, found 337.0854.

4.2.6.3.

*6-Chloro-2-(3-phenyl-1H-pyrazol-4-yl)quinazolin-4(3H)-one (**B5**)*

Off-white solid. Yield: 42%. Mp 286–288 °C. ^{1}H NMR (400 MHz, DMSO-d_6) δ 13.49 (s, 1H), 12.38 (s, 1H), 8.35–8.25 (m, 1H), 8.04 (d, J = 3.0 Hz, 1H), 7.77–7.75 (m, 1H), 7.70–7.68 (m, 2H), 7.43–7.41 (m, 4H). ^{13}C NMR (101 MHz, DMSO-d_6) δ 161.6, 149.6, 148.2, 134.9, 130.6, 129.6, 129.3, 128.4, 125.2, 122.4, 113.0. HRMS (ESI– TOF$^+$) calcd for $C_{17}H_{12}N_4OCl$ $[M+H]^+$ *m/z* 323.0700, found 323.0699.

4.2.6.4.

*8-Methyl-2-(3-phenyl-1H-pyrazol-4-yl)quinazolin-4(3H)-one (**B6**)*

Off-white solid. Yield: 49%. Mp 252–254 °C. ^{1}H NMR (400 MHz, DMSO-d_6) δ 13.57 (s, 0.5H), 13.39 (s, 0.5H), 12.22 (s, 1H), 8.54 (s, 0.5H), 8.29 (s, 0.5H), 7.93 (d, J = 7.7 Hz, 1H), 7.70 (dd, J = 7.5, 1.8 Hz, 2H), 7.56 (d, J = 7.1 Hz, 1H), 7.45–7.38 (m, 3H), 7.30 (t, J = 17.6 Hz, 1H), 2.14 (s, 3H). ^{13}C NMR (101 MHz, DMSO-d_6) δ 162.9, 148.0, 147.7, 135.6, 135.1, 129.5, 128.3, 125.8, 123.8, 121.1, 113.4, 17.4. HRMS (ESI–TOF$^+$) calcd for $C_{18}H_{15}N_4O$ $[M+H]^+$ *m/z* 303.1246, found 303.1257.

4.2.6.5.

*6, 8-Dimethyl-2-(3-phenyl-1H-pyrazol-4-yl)quinazolin-4(3H)-one (**B7**)*

Off-white solid. Yield: 41%. Mp 274–276 °C. ^{1}H NMR (400 MHz, DMSO-d_6) δ 13.53 (s, 0.5H), 13.37 (s, 0.5H), 12.12 (s, 1H), 8.51 (s, 0.5H), 8.26 (s, 0.5H), 7.73–7.68 (m, 3H), 7.45–7.34 (m, 4H), 2.37 (s, 3H), 2.13 (s, 3H). ^{13}C NMR (101 MHz, DMSO-d_6) δ 162.8, 146.9, 146.0, 136.4, 135.5, 135.3, 130.0, 128.3, 123.2, 120.9, 113.5, 21.2, 17.3. HRMS (ESI–TOF$^+$) calcd for $C_{19}H_{17}N_4O$ $[M+H]^+$ *m/z* 317.1402, found 317.1396.

4.2.6.6.

*2-(3-Phenyl-1H-pyrazol-4-yl)pyrido[2,3-d]pyrimidin-4(3H)-one (**B8**)*

Off-white solid. Yield: 40%. Mp 269–271 °C. ^{1}H NMR (400 MHz, DMSO-d_6) δ 13.62 (s, 0.5H), 13.51 (s, 0.5H), 12.49 (s, 1H), 8.88 (d, J = 6.6 Hz, 1H), 8.49–8.24 (m, 2H), 7.74–7.72 (m, 2H), 7.49–7.41 (m, 4H). ^{13}C NMR (101 MHz, DMSO-d_6) δ 163.2, 159.5, 156.3, 152.4, 135.8, 129.2, 128.5, 122.2, 116.3, 113.0. HRMS (ESI–TOF$^+$) calcd for $C_{16}H_{12}N_5O$ $[M+H]^+$ *m/z* 290.1042, found 290.1042.

4.2.7. General procedure for the synthesis of compounds ***C1-C6***

A mixture of 1*H*-imidazole-4-carbaldehyde (192 mg, 2 mmol), **7a-7e** (3 mmol), anhydrous Na_2CO_3 (424 mg, 4 mmol) and *tetra*-n-butylammonium iodide (74 mg, 0.2 mmol) in dry THF (10 mL) was refluxed for 3 h, and the solvent was removed under reduced pressure. The residue was extracted with EtOAc three times, and the combined organic layers were washed with brine, dried over anhydrous Na_2SO_4, filtered and concentrated. The crude product was purified by silica gel column chromatography eluting with CH_2Cl_2/MeOH (30/1) to afford **8a-8e**.

Cyanuric chloride (28 mg, 0.15 mmol) was added to a mixture of **3a** (136 mg, 1 mmol) and **8a-8e** (1.2 mmol) in DMSO (3 mL). The mixture was stirred at room temperature for 0.5-2 h. After completion, the mixture was extracted with EtOAc three times. The combined organic layers were washed with brine, dried over anhydrous Na_2SO_4, filtered and concentrated under reduced pressure. The crude product was purified by silica gel column chromatography eluting with CH_2Cl_2/MeOH (30/1) to afford **C1-C6**.

4.2.7.1.

*2-(1-Benzyl-1H-imidazol-4-yl)-2,3-dihydroquinazolin-4(1H)-one (**C1**)*

Off-white solid. Yield: 58%. Mp 189–191 °C. ^{1}H NMR (400 MHz, DMSO-d_6) δ 8.08 (s, 1H), 7.74 (s, 1H), 7.58 (d, J = 6.1 Hz, 1H), 7.37–7.26 (m, 5H), 7.20 (t, J = 7.6 Hz, 1H), 7.10 (s, 1H), 6.96 (s, 1H), 6.73 (d, J = 6.2 Hz, 1H), 6.64 (t, J = 7.4 Hz, 1H), 5.59 (s, 1H), 5.15 (s, 2H). ^{13}C NMR (101 MHz, DMSO-d_6) δ 164.0, 148.3, 143.0, 138.0, 137.7, 133.5, 129.1, 128.3, 128.2, 127.7, 117.4, 117.3, 115.6, 115.0, 62.5, 50.1. HRMS (ESI–TOF$^+$) calcd for $C_{18}H_{17}N_4O$ $[M+H]^+$ *m/z* 305.1402, found 305.1403.

4.2.7.2.

*2-(1-(3-Chlorobenzyl)-1H-imidazol-4-yl)-2,3-dihydroquinazolin-4(1H)-one (**C2**)*

Off-white solid. Yield: 58%. Mp 243–245 °C. ^{1}H NMR (400 MHz, DMSO-d_6) δ 8.12 (s, 1H), 7.77 (s, 1H), 7.60 (d, J = 7.1 Hz, 1H), 7.37 (s, 3H), 7.25–7.19 (m, 2H), 7.15 (s, 1H), 6.97 (s, 1H), 6.74 (d, J = 8.1 Hz, 1H), 6.65 (t, J = 7.5 Hz, 1H), 5.61 (s, 1H), 5.17 (s, 2H). ^{13}C NMR (101 MHz, DMSO-d_6) δ 164.0, 148.3, 143.1, 140.6, 137.8, 133.7, 133.5, 131.0, 128.2, 128.1, 127.7, 126.9, 117.4, 117.3, 115.6, 115.0, 62.4, 49.3. HRMS (ESI–TOF$^+$) calcd for $C_{18}H_{16}N_4OCl$ $[M+H]^+$ *m/z* 339.1007, found 339.1011.

4.2.7.3.

*2-(1-(4-Methoxybenzyl)-1H-imidazol-4-yl)-2,3-dihydroquinazolin-4(1H)-one (**C3**)*

Off-white solid. Yield: 59%. Mp 171–173 °C. ^{1}H NMR (400 MHz, DMSO-d_6) δ 8.06 (s, 1H), 7.71 (s, 1H), 7.60 (d, J = 7.6 Hz, 1H), 7.26–7.18 (m, 3H), 7.08 (s, 1H), 6.92 (t, J = 8.8 Hz, 3H), 6.74 (d, J = 8.1 Hz, 1H), 6.65 (t, J = 7.4 Hz, 1H), 5.59 (s, 1H), 5.06 (s, 2H), 3.74 (s, 3H). ^{13}C NMR (101 MHz, DMSO-d_6) δ 164.0, 159.4, 148.3, 142.9, 137.4, 133.5, 129.9, 129.8, 127.7, 117.3, 117.0, 115.6, 115.0, 114.5, 62.5, 55.6, 49.6. HRMS (ESI–TOF$^+$) calcd for $C_{19}H_{19}N_4O_2$ $[M+H]^+$ *m/z* 335.1505, found 335.1508.

4.2.7.4.

*2-(1-(4-Aminobenzyl)-1H-imidazol-4-yl)-2,3-dihydroquinazolin-4(1H)-one (**C4**)*

Off-white solid. Yield: 54%. Mp 159–161 °C. ^{1}H NMR (400 MHz, DMSO-d_6) δ 8.04 (s, 1H), 7.65 (s, 1H), 7.58 (d, J = 7.4 Hz, 1H), 7.19 (t, J = 8.6 Hz, 1H), 7.03 (s, 1H), 6.97 (d, J = 8.0 Hz, 2H), 6.93 (s, 1H), 6.72 (d, J = 8.7 Hz, 1H), 6.64 (t, J = 6.6 Hz, 1H), 6.50 (d, J = 8.0 Hz, 2H), 5.56 (s, 1H), 5.11 (s, 2H), 4.90 (s, 2H). ^{13}C NMR (101 MHz, DMSO-d_6) δ 164.0, 148.9, 148.3, 142.7, 137.2, 133.5, 129.5, 127.7, 124.5, 117.3, 116.9, 115.6, 115.0, 114.2, 62.5, 50.0. HRMS (ESI–TOF$^+$) calcd for $C_{18}H_{18}N_5O$ $[M+H]^+$ *m/z* 320.1511, found 320.1512.

4.2.7.5.

*2-(1-(4-Bromobenzyl)-1H-imidazol-4-yl)-2,3-dihydroquinazolin-4(1H)-one (**C5**)*

Off-white solid. Yield: 52%. Mp 215–217 °C. ^{1}H NMR (400 MHz, DMSO-d_6) δ 8.07 (s, 1H), 7.74 (s, 1H), 7.60–7.54 (m, 3H), 7.24–7.19 (m, 3H), 7.11 (s, 1H), 6.94 (s, 1H), 6.74 (d, J = 8.0 Hz, 1H), 6.65 (t, J = 7.4 Hz, 1H), 5.59 (s, 1H), 5.14 (s, 2H). ^{13}C NMR (101 MHz, DMSO-d_6) δ 164.0, 148.3, 143.1, 137.7, 137.5, 133.5, 132.0, 130.4, 127.7, 121.5, 117.3, 117.2, 115.6, 115.0, 62.4, 49.3. HRMS (ESI–TOF$^+$) calcd for $C_{18}H_{16}N_4OBr$ $[M+H]^+$ *m/z* 383.0502, found 383.0509.

4.2.7.6.

*2-(1-(4-Chlorobenzyl)-1H-imidazol-4-yl)-2,3-dihydroquinazolin-4(1H)-one (**C6**)*

Off-white solid. Yield: 52%. Mp 223–225 °C. ^{1}H NMR (400 MHz, DMSO-d_6) δ 8.05 (s, 1H), 7.74 (s, 1H), 7.59 (d, J = 7.1 Hz, 1H), 7.42 (d, J = 8.4 Hz, 2H), 7.30 (d, J = 8.4 Hz, 2H), 7.22–7.18(m, 1H), 7.11 (s, 1H), 6.94 (s, 1H), 6.73 (d, J = 8.0 Hz, 1H), 6.65 (t, J = 7.6 Hz, 1H), 5.59 (s, 1H), 5.16 (s, 2H). ^{13}C NMR (101 MHz, DMSO-d_6) δ 164.0, 148.3, 143.1, 137.7, 137.1, 133.5, 132.9, 130.1, 129.1, 127.7, 117.3, 117.2, 115.6, 115.0, 62.4, 49.2. HRMS (ESI–TOF$^+$) calcd for $C_{18}H_{16}N_4OCl$ $[M+H]^+$ *m/z* 339.1013, found 339.1011.

*4.2.8. The synthesis of compound **C7***

Cyanuric chloride (28 mg, 0.15 mmol) was added to a mixture of **3a** (136 mg, 1 mmol) and 1-(4-chlorobenzyl)-1*H*-imidazole-5-carbaldehyde (264 mg, 1.2 mmol) in DMSO (3 mL). The

mixture was stirred at room temperature for 2 h. After completion, the mixture was extracted with EtOAc three times. The combined organic layers were washed with brine, dried over anhydrous Na_2SO_4, filtered and concentrated under reduced pressure. The crude product was purified by silica gel column chromatography eluting with CH_2Cl_2/MeOH (30/1) to afford **C7**.

4.2.9.1.

*2-(1-(4-Chlorobenzyl)-1H-imidazol-5-yl)-2,3-dihydroquinazolin-4(1H)-one(**C7**)*

Off-white solid. Yield: 49%. Mp 233–235 °C. ^{1}H NMR (400 MHz, DMSO-d_6) δ 8.27 (s, 1H), 7.70 (s, 1H), 7.63 (dd, J = 7.8, 1.3 Hz, 1H), 7.42 (d, J = 8.5 Hz, 2H), 7.29–7.22 (m, 3H), 6.99 (s, 1H), 6.90 (s, 1H), 6.72 (dd, J = 17.1, 8.1 Hz, 2H), 5.80 (s, 1H), 5.37 (s, 2H). ^{13}C NMR (101 MHz, DMSO-d_6) δ 164.1, 147.9, 139.9, 136.7, 133.8, 132.8, 130.9, 129.7, 129.2, 129.1, 127.8, 118.2, 115.8, 115.3, 59.4, 47.8. HRMS (ESI–TOF$^+$) calcd for $C_{18}H_{16}N_4OCl$ $[M+H]^+$ *m/z* 339.1013, found 339.1012.

*4.2.9. The synthesis of compound **C8***

N-bromosuccinimide (561 mg, 3.15 mmol) was added as a single portion to a solution of pyrrole-2-carboxaldehyde (300 mg, 3.15 mmol) in THF (3.3 mL) at 0 °C. The mixture was stirred at 0 °C for 15 min, and the solvent was removed under reduced pressure. The crude product was suspended in water, the suspension was filtered, washed with water, recrystallized from EtOH and dried to afford 4-bromo-1*H*-pyrrole-2-carbaldehyde.

$Pd(PPh_3)_4$ (147 mg, 0.13 mol) was added to a degassed mixture of 4-bromo-1*H*-pyrrole-2-carbaldehyde (219 mg, 1.27 mmol), phenylboronic acid (221 mg, 1.81 mmol), K_2CO_3 (501mg, 3.63 mmol) in dioxane (4 mL) and water (2 mL) under argon. The mixture was heated at 105 °C for 24 h, cooled to room temperature and extracted with EtOAc three times. The combined organic layers were washed with brine, dried over anhydrous Na_2SO_4, filtered and concentrated under reduced pressure. The crude product was purified by silica gel column chromatography eluting with PE/EtOAc (6/1) to afford **9** [40].

Cyanuric chloride (28 mg, 0.15 mmol) was added to a mixture of **3a** (136 mg, 1 mmol) and **9** (205 mg, 1.2 mmol) in DMSO (3 mL). The mixture was stirred at room temperature for 2 h. After completion, the mixture was extracted with EtOAc three times. The combined organic layers were washed with brine, dried over anhydrous Na_2SO_4, filtered and concentrated under reduced pressure. The crude product was purified by silica gel column chromatography eluting with CH_2Cl_2/MeOH (30/1) to afford **C8**.

4.2.9.1.

*2-(4-Phenyl-1H-pyrrol-2-yl)-2,3-dihydroquinazolin-4(1H)-one (**C8**)*

Off-white solid. Yield: 38%. Mp 225–227 °C. ^{1}H NMR (400 MHz, DMSO-d_6) δ 11.16 (s, 1H), 8.13 (s, 1H), 7.64 (d, J = 6.0 Hz, 1H), 7.49 (d, J = 5.9 Hz, 2H), 7.30–7.23 (m, 4H), 7.09 (t, J = 7.3 Hz, 1H), 6.96 (s, 1H), 6.79–6.69 (m, 2H), 6.49 (s, 1H), 5.78 (s, 1H). ^{13}C NMR (101 MHz, DMSO-d_6) δ 164.3, 148.6, 136.3, 133.6, 132.6, 129.1, 127.9, 125.4, 124.8, 123.4, 117.8, 116.0, 115.7, 115.1, 105.3, 62.0. HRMS (ESI–TOF$^+$) calcd for $C_{18}H_{16}N_3O$ $[M+H]^+$ *m/z* 290.1293, found 290.1296.

*4.2.10. General procedure for the synthesis of compounds **D1-D12***

Cyanuric chloride (28 mg, 0.15 mmol) was added to a mixture of **3a**, **3b**, **3k** or **3s** (1 mmol) and **4b-4h** (1.2 mmol) in MeOH or DMSO (3 mL). The mixture was stirred at room temperature for 0.5-2 h. After completion, the mixture was extracted with EtOAc three times. The combined organic layers were washed with brine, dried over anhydrous Na_2SO_4, filtered and concentrated under reduced pressure. The crude product was purified by silica gel column chromatography eluting with CH_2Cl_2/MeOH (30/1) to afford **D1-D12**.

4.2.10.1.

*6-Chloro-8-methyl-2-(3-(naphthalen-1-yl)-1H-pyrazol-4-yl)-2,3-dihydroquinazolin-4(1H)-one (**D1**)*

MeOH was employed as the solvent. Off-white solid. Yield: 54%. Mp 155–157 °C. ^{1}H NMR (400 MHz, DMSO-d_6) δ 13.32 (s, 0.5H), 13.12 (s, 0.5H), 8.42 (s, 1H), 8.21–7.93 (m, 6H), 7.54–7.51 (m, 3H), 7.23 (s, 1H), 6.38 (s, 1H), 5.96 (s, 1H), 2.08 (s, 3H). ^{13}C NMR (101 MHz, DMSO-d_6) δ 163.6, 145.6, 133.7, 133.3, 132.8, 128.6, 128.4, 127.3, 126.6, 124.7, 121.7, 118.4, 117.5, 60.3, 17.1. HRMS (ESI–TOF$^+$) calcd for $C_{22}H_{18}N_4OCl$ $[M+H]^+$ *m/z* 389.1169, found 389.1162.

4.2.10.2.

*6-Chloro-8-methyl-2-(3-(4-nitrophenyl)-1H-pyrazol-4-yl)-2,3-dihydroquinazolin-4(1H)-one (**D2**)*

MeOH was employed as the solvent. Off-white solid. Yield: 56%. Mp 186–188 °C. ^{1}H NMR (400 MHz, DMSO-d_6) δ 13.55 (s, 0.2H), 13.35 (s, 0.8H), 8.41–8.27 (m, 3H), 8.05–7.88 (m, 3H), 7.49 (s, 1H), 7.25 (s, 1H), 6.39 (s, 1H), 5.91 (d, J = 36.2 Hz, 1H), 2.08 (s, 3H). ^{13}C NMR (101 MHz, DMSO-d_6) δ 163.7, 145.6, 133.7, 131.8, 129.4, 126.8, 124.7, 124.1, 121.8, 119.0, 60.2, 17.1. HRMS (ESI–TOF$^+$) calcd for $C_{18}H_{15}N_5O_3Cl$ $[M+H]^+$ *m/z* 384.0863, found 384.0863.

4.2.10.3.

*6-Chloro-8-methyl-2-(1H-pyrazol-4-yl)-2,3-dihydroquinazolin-4(1H)-one (**D3**)*

MeOH was employed as the solvent. Off-white solid. Yield: 50%. Mp 255–257 °C. ^{1}H NMR (400 MHz, DMSO-d_6) δ 8.40 (s, 1H), 7.57 (s, 2H), 87.44 (s, 1H), 7.21 (s, 1H), 6.53 (s, 1H), 5.75 (s, 1H), 2.12 (s, 3H). ^{13}C NMR (101 MHz, DMSO-d_6) δ 163.4, 145.1, 133.6, 126.1, 124.6, 122.7, 121.1, 117.0, 59.9, 17.1. HRMS (ESI–TOF^{+}) calcd for $C_{12}H_{12}N_4OCl$ $[M+H]^{+}$ *m/z* 263.0700, found 263.0702.

4.2.10.4.

*2-(3-(4-Chlorophenyl)-1H-pyrazol-4-yl)-2,3-dihydroquinazolin-4(1H)-one (**D4**)*

MeOH was employed as the solvent. Off-white solid. Yield: 70%. Mp 224–226 °C. ^{1}H NMR (400 MHz, DMSO-d_6) δ 13.31 (s, 0.4H), 13.15 (s, 0.6H), 8.15 (s, 1H), 8.05 (s, 0.5H), 7.76 (s, 0.5H), 7.74 (s, 1H), 7.66–7.57 (m, 2H), 7.48 (d, J = 8.3 Hz, 1H), 7.26 (t, J = 7.6 Hz, 1H), 6.92 (s, 1H), 6.76–6.72 (m, 2H), 5.80 (d, J = 36.3 Hz, 2H). ^{13}C NMR (101 MHz, DMSO-d_6) δ 164.6, 149.1, 148.2, 133.6, 133.0, 132.7, 130.8, 130.3, 129.3, 128.8, 128.0, 118.1, 117.8, 116.1, 115.2, 60.7. HRMS (ESI–TOF^{+}) calcd for $C_{17}H_{14}N_4OCl$ $[M+H]^{+}$ *m/z* 325.0851, found 325.0853.

4.2.10.5.

*2-(3-([1,1'-Biphenyl]-4-yl)-1H-pyrazol-4-yl)-6-chloro-8-methyl-2,3-dihydroquinazolin-4(1H)-one (**D5**)*

MeOH was employed as the solvent. Off-white solid. Yield: 62%. Mp 161–163 °C. ^{1}H NMR (400 MHz, DMSO-d_6) δ 13.29 (s, 0.5H), 13.10 (s, 0.5H), 8.42 (s, 1H), 8.01–7.71 (m, 7H), 7.50–7.37 (m, 4H), 7.25 (d, J = 1.9 Hz, 1H), 6.37 (s, 1H), 5.87 (s, 1H), 2.10 (s, 3H). ^{13}C NMR (101 MHz, DMSO-d_6) δ 163.7, 145.8, 133.7, 129.5, 129.1, 128.1, 127.1, 126.6, 124.7, 121.6, 117.9, 117.5, 60.4, 17.14. HRMS (ESI–TOF^{+}) calcd for $C_{24}H_{20}N_4OCl$ $[M+H]^{+}$ *m/z* 415.1326, found 415.1321.

4.2.10.6.

*2-(3-(2-Bromophenyl)-1H-pyrazol-4-yl)-6-chloro-8-methyl-2,3-dihydroquinazolin-4(1H)-one (**D6**)*

MeOH was employed as the solvent. Off-white solid. Yield: 52%. Mp 153–155 °C. ^{1}H NMR (400 MHz, DMSO-d_6) δ 8.28 (s, 1H), 7.79–7.69 (m, 2H), 7.44–7.35 (m, 4H), 7.16 (s, 1H), 6.07 (s, 1H), 5.60 (s, 1H), 1.94 (s, 3H). ^{13}C NMR (101 MHz, DMSO-d_6) δ 163.4, 144.9, 133.5, 133.0, 127.9, 126.5, 124.6, 124.0, 121.5, 119.8, 117.4, 59.9, 16.9. HRMS (ESI–TOF^{+}) calcd for $C_{18}H_{15}N_4OClBr$ $[M+H]^{+}$ *m/z* 417.0118, found 417.0119.

4.2.10.7.

*2-(3-(4-Bromophenyl)-1H-pyrazol-4-yl)-6-chloro-8-methyl-2,3-dihydroquinazolin-4(1H)-one (**D7**)*

MeOH was employed as the solvent. Off-white solid. Yield: 49%. Mp 271–273 °C. ^{1}H NMR (400 MHz, DMSO-d_6) δ 13.28 (s, 0.4H), 13.12 (s, 0.6H), 8.35 (s, 1H), 7.98–7.66 (m, 3H), 7.62–7.49 (m, 3H), 7.23 (s, 1H), 6.31 (s, 1H), 5.81 (d, J = 24.2 Hz, 1H), 2.08 (s, 3H). ^{13}C NMR (101 MHz, DMSO-d_6) δ 163.6, 145.7, 133.7, 131.8, 130.6, 126.6, 124.7, 121.7, 118.0, 117.5, 60.3, 17.1. HRMS (ESI–TOF$^+$) calcd for $C_{18}H_{15}N_4OClBr$ $[M+H]^+$ *m/z* 417.0118, found 417.0119.

4.2.10.8.

*6-Chloro-2-(3-(4-chlorophenyl)-1H-pyrazol-4-yl)-8-methyl-2,3-dihydroquinazolin-4(1H)-one (**D8**)*

MeOH was employed as the solvent. Off-white solid. Yield: 57%. Mp 281–283 °C. ^{1}H NMR (400 MHz, DMSO-d_6) δ 13.28 (s, 0.3H), 13.13 (s, 0.7H), 8.37 (s, 1H), 7.99–7.49 (m, 6H), 7.23 (s, 1H), 6.34 (s, 1H), 5,84 (s, 1H), 2.08 (s, 3H). ^{13}C NMR (101 MHz, DMSO-d_6) δ 163.6, 145.7, 133.7, 130.3, 128.9, 126.6, 124.7, 121.7, 118.0, 117.5, 60.3, 17.1. HRMS (ESI–TOF$^+$) calcd for $C_{18}H_{15}N_4OCl_2$ $[M+H]^+$ *m/z* 373.0623, found 373.0621.

4.2.10.9.

*6-Bromo-8-methyl-2-(3-(naphthalen-1-yl)-1H-pyrazol-4-yl)-2,3-dihydroquinazolin-4(1H)-one (**D9**)*

DMSO was employed as the solvent. Off-white solid. Yield: 47%. Mp 253–255 °C. ^{1}H NMR (400 MHz, DMSO-d_6) δ 13.33 (s, 0.5H), 13.12 (s, 0.5H), 8.41 (s, 1H), 8.19 (d, J = 31.7 Hz, 1H), 8.04–7.72 (m, 5H), 7.64 (s, 1H), 7.55 (d, J = 16.8 Hz, 2H), 7.35 (s, 1H), 6.40 (d, J = 8.9 Hz, 1H), 5.95 (d, J = 34.6 Hz, 1H), 2.08 (s, 3H). ^{13}C NMR (101 MHz, DMSO-d_6) δ 163.6, 146.0, 136.4, 133.3, 132.9, 128.6, 128.1, 127.8, 127.3, 126.9, 118.4, 117.9, 109.2, 60.3, 17.1. HRMS (ESI–TOF$^+$) calcd for $C_{22}H_{18}N_4OBr$ $[M+H]^+$ *m/z* 433.0664, found 433.0666.

4.2.10.10.

*6-Bromo-8-methyl-2-(3-(4-nitrophenyl)-1H-pyrazol-4-yl)-2,3-dihydroquinazolin-4(1H)-one (**D10**)*

DMSO was employed as the solvent. Yellow solid. Yield: 52%. Mp 189–191 °C. ^{1}H NMR (400 MHz, DMSO-d_6) δ 13.54 (s, 0.8H), 13.34 (s, 0.8H), 8.39–8.27 (m, 3H), 8.04–7.76 (m, 3H), 7.63 (s, 1H), 7.36 (s, 1H), 6.40 (s, 1H), 5.92 (d, J = 33.4 Hz, 1H), 2.07 (s, 3H). ^{13}C NMR (101 MHz, DMSO-d_6) δ 163.6, 146.0, 136.4, 131.3, 129.4, 127.8, 127.1, 124.0, 119.0, 118.0, 109.3, 60.2, 17.1. HRMS (ESI–TOF$^+$) calcd for $C_{18}H_{15}N_5O_3Br$ $[M+H]^+$ *m/z* 428.0358, found 428.0353.

4.2.10.11.

*6-Chloro-8-iodo-2-(3-(naphthalen-1-yl)-1H-pyrazol-4-yl)-2,3-dihydroquinazolin-4(1H)-one (**D11**)*

DMSO was employed as the solvent. Off-white solid. Yield: 55%. Mp 202–204 °C. ^{1}H NMR (400 MHz, DMSO-d_6) δ 13.36 (s, 0.5H), 13.11 (s, 0.5H), 8.72 (s, 1H), 8.23 (d, J = 28.0 Hz, 1H), 8.06–7.92 (m, 4H), 7.87–7.77 (m, 2H), 7.68 (d, J = 2.2 Hz, 1H), 7.57 (d, J = 20.4 Hz, 2H), 6.08 (d, J

= 31.7 Hz, 2H). ^{13}C NMR (101 MHz, DMSO-d_6) δ 162.4, 146.7, 141.7, 133.5, 132.9, 128.6, 128.0, 127.6, 127.1, 126.7, 123.3, 118.8, 86.4, 60.1. HRMS (ESI–TOF$^+$) calcd for $C_{21}H_{15}N_4OClI$ $[M+H]^+$ *m/z* 500.9979, found 500.9981.

4.2.10.12.

*6-Chloro-8-iodo-2-(3-(4-nitrophenyl)-1H-pyrazol-4-yl)-2,3-dihydroquinazolin-4(1H)-one (**D12**)*

DMSO was employed as the solvent. Off-white solid. Yield: 49%. Mp 289–291 °C. ^{1}H NMR (400 MHz, DMSO-d_6) δ 13.54 (s, 0.2H), 13.29 (s, 0.8H), 8.70 (s, 1H), 8.36–8.28 (m, 2H), 8.03–7.90 (m, 3H), 7.84 (s, 1H), 7.64 (d, J = 10.7 Hz, 1H), 6.15–5.99 (m, 2H). ^{13}C NMR (101 MHz, DMSO-d_6) δ 162.3, 146.7, 141.7, 130.8, 129.4, 127.5, 124.1, 123.4, 119.8, 118.3, 86.5, 59.9. HRMS (ESI–TOF$^+$) calcd for $C_{17}H_{12}N_5O_3ClI$ $[M+H]^+$ *m/z* 495.9673, found 495.9659.

*4.3. Chiral resolution and absolute configuration of **A1***

4.3.1. Chiral resolution and analyses

Chiral resolution of **A1** was achieved by using chiral chromatographic resolution. Racemic **A1** was separated on a ChiralPak AD-H column (250 mm, 10 mm, 5 μm, Daicel Inc.) with n-hexane/isopropanol, 85:15, as eluent. A solution of **A1** (ca. 0.20 mg) in MeOH (0.2 mL) was loaded for each batch and eluted at a flow rate of 3.0 mL min^{-1}. The enantiomers were eluted and collected at 20.81 min and 25.51 min, respectively. Analytical enantiomeric resolution was then carried out on a ChiralPak AD-H column (250 mm, 4.6 mm, 5 μm, Daicel Inc.) with a mixture of n-hexane and ethanol 70:30 as the mobile phase to determine the purity of enantiomers. Optical rotations were measured on a Rudolph Autopol IV polarimeter with an optical path of 50 mm at 20 °C with the compounds dissolved in MeOH.

4.3.2. ECD measurements

ECD measurements were obtained with a Jasco J-810 CD spectrometer. The CD spectra of each enantiomer was measured in the 200-400 nm range using 0.1 cm pathlength quartz cuvettes with the continuous mode under the following conditions: scan rate 100 nm/min, bandwidth 1 nm, response time 1 s, 3 accumulations.

4.3.3. ECD calculations

The ECD calculations of **R-A1** and **S-A1** were mainly referred to literature method *[42]*

Preliminary conformational analysis was performed in SYBYL-X 1.1 using random search method with the MMFF94 force field. Conformers within 6 kcal/mol were saved and further optimized using the density functional theory (DFT) method at the B3LYP/6-31G* level. Frequency was calculated at the same level of theory. The stable conformers with populations greater than 1%

and without imaginary frequencies were submitted to ECD calculation by the TDDFT [B3LYP/6-31G*] method. Considering solvent effects on calculation, IEFPCM model in MeOH was used in this study. ECD spectra for each conformer was simulated using SpecDis. The final ECD spectra were generated according to the Boltzmann-calculated distribution of each conformer. All calculations were performed with Gaussian 09 program package.

4.3.4. Enantiomers characterization

4.3.4.1.

*(R)-6-Chloro-8-methyl-2-(3-phenyl-1H-pyrazol-4-yl)-2,3-dihydroquinazolin-4(1H)-one (**R-A1**)*

Off-white solid. Mp 175–177 °C. $[\alpha]_D^{20}$ = -165.3 (c = 0.1 in MeOH). t_R = 20.81 min (preparative chromatography), 11.64 min (analytical chromatograph). ECD (MeOH) λ_{max} ($\Delta\varepsilon$) = 221 (+9.19), 237 (-9.66), 252 (-8.60), 351 (-2.20) nm. ^{1}H NMR (400 MHz, DMSO-d_6) δ 13.21 (s, 0.5H), 13.06 (s, 0.5H), 8.37 (s, 1H), 7.69–7.63 (m, 3H), 7.50–7.37 (m, 4H), 7.23 (d, J = 1.8 Hz, 1H), 6.31 (s, 1H), 5.81 (d, J = 13.5 Hz, 1H), 2.08 (s, 3H). ^{13}C NMR (101 MHz, DMSO-d_6) δ 163.6, 145.7, 133.7, 129.6, 128.6, 126.6, 124.7, 121.6, 117.9, 117.5, 60.3, 17.1. HRMS (ESI–TOF$^+$) calcd for $C_{18}H_{16}N_4OCl$ $[M+H]^+$ *m/z* 339.1013, found 339.1013.

4.3.4.2.

*(S)-6-Chloro-8-methyl-2-(3-phenyl-1H-pyrazol-4-yl)-2,3-dihydroquinazolin-4(1H)-one (**S-A1**)*

Off-white solid. Mp 175–177 °C. $[\alpha]_D^{20}$ = +164.0 (c = 0.1 in MeOH). t_R = 25.51 min (preparative chromatography), 10.71 min (analytical chromatograph). ECD (MeOH) λ_{max} ($\Delta\varepsilon$) = 219 (-6.86), 237 (+7.00), 251 (+6.40), 349 (+1.84) nm. ^{1}H NMR (400 MHz, DMSO-d_6) δ 13.22 (s, 0.5H), 13.06 (s, 0.5H), 8.38 (s, 1H), 7.69–7.62 (m, 3H), 7.49–7.36 (m, 4H), 7.23 (s, 1H), 6.30 (s, 1H), 5.79 (d, J = 34.6 Hz, 1H), 2.07 (s, 3H). ^{13}C NMR (101 MHz, DMSO-d_6) δ 163.6, 145.7, 133.7, 128.9, 128.6, 126.6, 124.7, 121.6, 117.7, 117.5, 60.3, 17.1. HRMS (ESI–TOF$^+$) calcd for $C_{18}H_{16}N_4OCl$ $[M+H]^+$ *m/z* 339.1013, found 339.1010.

4.4. Cell culture and transfection

The tetracycline-inducible human embryonic kidney (HEK) 293 cells were maintained in DMEM/F-12 (Gibco, USA) containing 10% fetal bovine serum (FBS) and 1 μg/mL tetracycline (Sigma, USA) as described previously [32,33]. HEK293 cells were used to transiently express the wild-type TRPM8. One ug Human TRPM8 (NCBI Reference Sequence: NM_024080.4, in pcDNA4/TO vector), and 50 ng green fluorescent protein were together transfected into HEK293 cells using Lipofectamine 2000 for 24~48 h before recordings. All cells were cultured at 37 °C under a humidified atmosphere containing 5% CO_2. Cells were seeded on coverslips before use.

4.5. Calcium measurements

Free $[Ca^{2+}]_i$ was determined using Fluo-3/AM (Life Technologies, USA) as described previously [44]. Cells in 96-well plates (3603; Costar) were incubated with 3.5 μM Fluo-3/AM at 37 °C for 0.5 h, and washed with Hanks' balanced salt solution (HBSS) and the fluorescence intensity was measured using a full-wavelength multifunction scanning reader (Thermo Scientific, USA) with excitation at 485 nm and emission at 525 nm. The intensity of the control well, in which 1 mM H_2O_2 was added, was set as 100% and the data were normalized as percentages of the control. Each group had 3 replicate wells and all procedures were performed in dark.

4.6. Electrophysiology

For inhibitory activity test on the TRPM2 channel, patch-clamp recordings were performed in whole-cell configuration at room temperature using Axonpatch 200B (Axon, CNS). Similar to our previously reported protocol [28], cells were kept in extracellular solution (ECS) containing (in mM): 145 NaCl, 5.6 KCl, 2$MgCl_2$, 1.2 $CaCl_2$, 10 HEPES, pH 7.2. Electrodes had a final resistance of 3–5 MΩ when filled with intracellular solution (ICS) containing (in mM): 147 NaCl, 1 EGTA, 1 $MgCl_2$, 24 HEPES, pH 7.3. Patch pipettes were prepared from the Narishige PC-10 puller (Narishige, Japan) with Borosilicate glass (Sutter, USA). The ADPR concentration was fixed at 500 μM in the ICS. Test compounds were added to ECS with indicated concentrations and perfused for at least 60 s after the ADPR activated TRPM2 current got stable. Acidic ECS (pH 5.0) was applied to block TRPM2 currents. Change of ECS was achieved using an RSC-160 system (Biologic Science Instruments, France) in which the solution changing time was about 300 ms. Cell was held at 0 mV. Voltage ramps with 500 ms duration from −100 to 100 mV were applied every 5 s. Data were acquired at 10 kHz and filtered offline at 50 Hz. Mean of the first three ramps before channel activation was used for leak subtraction of all current recordings. The cells chose to calculate should satisfy two conditions: 1) the leak current of chose cells is less than 100pA at -80mV after whole cell configuration; 2) the remained current after pH5.0 treatment is also less than 100pA at -80mV.

For specificity evaluation, recordings were carried out on the TRPM8 currents. The ECS contains (in mM): 130 NaCl, 5 KCl, 10 D-glucose, 10 HEPES, 1.2 $MgCl_2$ and 1.5 $CaCl_2$, pH 7.4. The ICS contains (in mM): 115 CsCl, 10 EGTA, 2 $MgCl_2$, 10 HEPES and 5.7 $CaCl_2$, pH 7.2. The test compounds (30 μM) were added to either ECS or ICS to determine their effects on the TRPM8 currents. Menthol (1 mM) was added in ECS to activate TRPM8, and 2-APB (0.1 mM) was applied in ECS to inhibit TRPM8.

4.7 Data analysis

Calcium measurements from at least three independent experiments and electrophysiological recordings from at least five cells were averaged and presented in the text and figures, where appropriate, as means ± SEM. Statistical analysis was performed using two-tailed paired Student's *t* test for comparison between groups, with $P < 0.05$ considered to be statistically significant. GraphPad Prism 6 software was used for all statistical analyses.

4.8. Virtual screening

4.8.1. Preparation of compound library

In brief, SPECS and PKU_CNCL [45] databases were prepared by a homemade protocol in Pipeline Pilot v7.5 (PP 7.5, Accelrys, Inc.), in which the molecules formed 3D coordinates. The two prepared databases were filtered by a basic standard in FILTER (OpenEye Scientific Software, Inc) to eliminate molecules with unsatisfied properties. Subsequently, the databases were prepared with OMEGA (OpenEye Scientific Software, Inc) to generate up to 500 conformations for each molecule.

4.8.2. Similarity search

For shape-based 3D similarity search, 3D structures of AMP were generated and energy minimized by using LigPrep module of Schrödinger Suite (Schrödinger, LLC, New York, NY, USA). The optimized conformation of AMP was used to generate ROCS query using ROCS 3.1.2. During the process, the Max. Molecules Per Model and the Models to Keep were set to 5. The query model was used to search the two prepared databases. The results were ranked by 'Shape Tanimoto' score and the top 3,000 (2×3,000) compounds were retained.

ROCS output compounds were used as input for electrostatic-based analysis using EON 2.1.0, which calculate the electrostatic distribution similarity between each molecule and the query. New partial charges for the input structures were computed using MMFF94. The output files were then ranked by the 'ET_pb' score, and the top 300 (2×300) compounds were retained.

After removing the duplicated compounds, cluster analysis was performed on the retained compounds using PP 7.5. ECFP-6 was chosen to be molecular fingerprint. Finally, 24 compounds were selected and purchased from the commercial source for biological evaluation.

Acknowledgments

This research work was financially supported by National Natural Science Foundation of China (NSFC 81573273, NSFC 81673279, NSFC 81571127 and NSFC 21402171) and Zhejiang Provincial Natural Science Foundation of China under Grant No. LR16H090001.

References

[1] Y. Kaneko, A. Szallasi, Transient receptor potential (TRP) channels: a clinical perspective, Br. J. Pharmacol., 171 (2014) 2474-2507.

[2] B. Nilius, A. Szallasi, Transient receptor potential channels as drug targets: from the science of basic research to the art of medicine, Pharmacol. Rev., 66 (2014) 676-814.

[3] K. Venkatachalam, C. Montell, TRP channels, Annu. Rev. Biochem, 76 (2007) 387-417.

[4] A. Fleig, R. Penner, The TRPM ion channel subfamily: molecular, biophysical and functional features, Trends Pharmacol. Sci, 25 (2004) 633-639.

[5] H. Knowles, Y. Li, A.L. Perraud, The TRPM2 ion channel, an oxidative stress and metabolic sensor regulating innate immunity and inflammation, Immunol. Res., 55 (2013) 241-248.

[6] A. Sumoza-Toledo, R. Penner, TRPM2: a multifunctional ion channel for calcium signalling, J. Physiol., 589 (2011) 1515-1525.

[7] K. Song, H. Wang, G.B. Kamm, J. Pohle, F.C. Reis, P. Heppenstall, H. Wende, J. Siemens, The TRPM2 channel is a hypothalamic heat sensor that limits fever and can drive hypothermia, Science, 353 (2016) 1393-1398.

[8] C.H. Tan, P.A. McNaughton, The TRPM2 ion channel is required for sensitivity to warmth, Nature, 536 (2016) 460-463.

[9] K.Y. Zhan, P.L. Yu, C.H. Liu, J.H. Luo, W. Yang, Detrimental or beneficial: the role of TRPM2 in ischemia/reperfusion injury, Acta Pharmacol. Sin., 37 (2016) 4-12.

[10] K. Uchida, M. Tominaga, The role of TRPM2 in pancreatic beta-cells and the development of diabetes, Cell Calcium, 56 (2014) 332-339.

[11] J. Wang, M.F. Jackson, Y.F. Xie, Glia and TRPM2 Channels in Plasticity of Central Nervous System and Alzheimer's Diseases, Neural Plast., 1 (2016) 1-7.

[12] H. Watanabe, M. Murakami, T. Ohba, Y. Takahashi, H. Ito, TRP channel and cardiovascular disease, Pharmacol. Ther., 118 (2008) 337-351.

[13] R. Yonezawa, S. Yamamoto, M. Takenaka, Y. Kage, T. Negoro, T. Toda, M. Ohbayashi, T. Numata, Y. Nakano, T. Yamamoto, Y. Mori, M. Ishii, S. Shimizu, TRPM2 channels in alveolar epithelial cells mediate bleomycin-induced lung inflammation, Free Radic. Biol. Med., 90 (2016) 101-113.

[14] M. Ye, W. Yang, J.F. Ainscough, X.P. Hu, X. Li, A. Sedo, X.H. Zhang, X. Zhang, Z. Chen, X.M. Li, D.J. Beech, A. Sivaprasadarao, J.H. Luo, L.H. Jiang, TRPM2 channel deficiency prevents delayed cytosolic Zn2+ accumulation and CA1 pyramidal neuronal death after transient global ischemia, Cell Death Dis., 5 (2014) e1541.

[15] K. So, K. Haraguchi, K. Asakura, K. Isami, S. Sakimoto, H. Shirakawa, Y. Mori, T. Nakagawa, S. Kaneko, Involvement of TRPM2 in a wide range of inflammatory and neuropathic pain mouse models, J. Pharmacol. Sci., 127 (2015) 237-243.

[16] A.L. Perraud, A. Fleig, C.A. Dunn, L.A. Bagley, P. Launay, C. Schmitz, A.J. Stokes, Q. Zhu, M.J. Bessman, R. Penner, J.P. Kinet, A.M. Scharenberg, ADP-ribose gating of the calcium-permeable LTRPC2 channel revealed by Nudix motif homology, Nature, 411 (2001) 595-599.

[17] P. Yu, X. Xue, J. Zhang, X. Hu, Y. Wu, L.H. Jiang, H. Jin, J. Luo, L. Zhang, Z. Liu, W. Yang, Identification of the ADPR binding pocket in the NUDT9 homology domain of TRPM2, J. Gen. Physiol., 149 (2017) 219-235.

[18] N. Takahashi, D. Kozai, R. Kobayashi, M. Ebert, Y. Mori, Roles of TRPM2 in oxidative stress, Cell Calcium, 50 (2011) 279-287.

[19] K. Hill, S. McNulty, A.D. Randall, Inhibition of TRPM2 channels by the antifungal agents clotrimazole and econazole, Naunyn Schmiedebergs Arch. Pharmacol., 370 (2004) 227-237.
[20] M. Naziroglu, A. Luckhoff, E. Jungling, Antagonist effect of flufenamic acid on TRPM2 cation channels activated by hydrogen peroxide, Cell Biochem. Funct., 25 (2007) 383-387.
[21] G.L. Chen, B. Zeng, S. Eastmond, S.E. Elsenussi, A.N. Boa, S.Z. Xu, Pharmacological comparison of novel synthetic fenamate analogues with econazole and 2-APB on the inhibition of TRPM2 channels, Br. J. Pharmacol., 167 (2012) 1232-1243.
[22] R. Kraft, C. Grimm, H. Frenzel, C. Harteneck, Inhibition of TRPM2 cation channels by N-(p-amylcinnamoyl)anthranilic acid, Br. J. Pharmacol., 148 (2006) 264-273.
[23] K. Togashi, H. Inada, M. Tominaga, Inhibition of the transient receptor potential cation channel TRPM2 by 2-aminoethoxydiphenyl borate (2-APB), Br. J. Pharmacol., 153 (2008) 1324-1330.
[24] M. Kolisek, A. Beck, A. Fleig, R. Penner, Cyclic ADP-ribose and hydrogen peroxide synergize with ADP-ribose in the activation of TRPM2 channels, Mol. Cell, 18 (2005) 61-69.
[25] I. Lange, R. Penner, A. Fleig, A. Beck, Synergistic regulation of endogenous TRPM2 channels by adenine dinucleotides in primary human neutrophils, Cell Calcium, 44 (2008) 604-615.
[26] S. Partida-Sanchez, A. Gasser, R. Fliegert, C.C. Siebrands, W. Dammermann, G. Shi, B.J. Mousseau, A. Sumoza-Toledo, H. Bhagat, T.F. Walseth, A.H. Guse, F.E. Lund, Chemotaxis of mouse bone marrow neutrophils and dendritic cells is controlled by adp-ribose, the major product generated by the CD38 enzyme reaction, J. Immunol., 179 (2007) 7827-7839.
[27] C. Moreau, T. Kirchberger, J.M. Swarbrick, S.J. Bartlett, R. Fliegert, T. Yorgan, A. Bauche, A. Harneit, A.H. Guse, B.V. Potter, Structure-activity relationship of adenosine 5'-diphosphoribose at the transient receptor potential melastatin 2 (TRPM2) channel: rational design of antagonists, J. Med. Chem., 56 (2013) 10079-10102.
[28] X. Luo, M. Li, K. Zhan, W. Yang, L. Zhang, K. Wang, P. Yu, L. Zhang, Selective inhibition of TRPM2 channel by two novel synthesized ADPR analogues, Chem. Biol. Drug Des., (2017).
[29] J.M. Swarbrick, A.M. Riley, S.J. Mills, B.V. Potter, Designer small molecules to target calcium signalling, Biochem. Soc. Trans., 43 (2015) 417-425.
[30] J.G. Starkus, P. Poerzgen, K. Layugan, K.G. Kawabata, J.I. Goto, S. Suzuki, G. Myers, M. Kelly, R. Penner, A. Fleig, F.D. Horgen, Scalaradial Is a Potent Inhibitor of Transient Receptor Potential Melastatin 2 (TRPM2) Ion Channels, J. Nat. Prod., 80 (2017) 2741-2750.
[31] A. Nicholls, G.B. McGaughey, R.P. Sheridan, A.C. Good, G. Warren, M. Mathieu, S.W. Muchmore, S.P. Brown, J.A. Grant, J.A. Haigh, N. Nevins, A.N. Jain, B. Kelley, Molecular shape and medicinal chemistry: a perspective, J. Med. Chem., 53 (2010) 3862-3886.
[32] W. Yang, J. Zou, R. Xia, M.L. Vaal, V.A. Seymour, J. Luo, D.J. Beech, L.-H. Jiang, State-dependent inhibition of TRPM2 channel by acidic pH, J. Biol. Chem., 285 (2010) 30411-30418.
[33] W. Yang, P.T. Manna, J. Zou, J. Luo, D.J. Beech, A. Sivaprasadarao, L.-H. Jiang, Zinc inactivates melastatin transient receptor potential 2 channels via the outer pore, J. Biol. Chem., 286 (2011) 23789-23798.
[34] W. Yu, L.H. Jiang, Y. Zheng, X. Hu, J. Luo, W. Yang, Inactivation of TRPM2 Channels by Extracellular Divalent Copper, PLoS One, 9 (2014) e112071.
[35] A. Nathubhai, T. Haikarainen, P.C. Hayward, S. Munoz-Descalzo, A.S. Thompson, M.D. Lloyd, L. Lehtio, M.D. Threadgill, Structure-activity relationships of 2-arylquinazolin-4-ones as highly selective and potent inhibitors of the tankyrases, Eur. J. Med. Chem., 118 (2016) 316-327.
[36] M. Sharma, S. Pandey, K. Chauhan, D. Sharma, B. Kumar, P.M. Chauhan, Cyanuric chloride catalyzed mild protocol for synthesis of biologically active dihydro/spiro quinazolinones and quinazolinone-glycoconjugates, J. Org. Chem., 77 (2012) 929-937.

[37] V.B. Labade, P.V. Shinde, M.S. Shingare, A facile and rapid access towards the synthesis of 2,3-dihydroquinazolin-4(1H)-ones, Tetrahedron Lett., 54 (2013) 5778-5780.
[38] S.K. Kumar, D. Rambabu, C.H.V. Kumar, B.Y. Sreenivas, K.R.S. Prasad, M.V.B. Rao, M. Pal, Catalysis by Amberlyst-15 under ultrasound in water: a green synthesis of 1,2,4-benzothiadiazine-1,1-dioxides and their spiro derivatives, RSC Advances, 3 (2013) 24863-24867.
[39] R. Salvio, R. Cacciapaglia, L. Mandolini, General base-guanidinium cooperation in bifunctional artificial phosphodiesterases, J. Org. Chem., 76 (2011) 5438-5443.
[40] V.K. Outlaw, F.B. d'Andrea, C.A. Townsend, One-pot synthesis of highly substituted N-fused heteroaromatic bicycles from azole aldehydes, Org. Lett., 17 (2015) 1822-1825.
[41] A.V. Lebedev, A.B. Lebedeva, V.D. Sheludyakov, E.A. Kovaleva, O.L. Ustinova, I.B. Kozhevnikov, Synthesis of 3-substituted arylpyrazole-4-carboxylic acids, Russ. J. Gen. Chem., 75 (2005) 782-789.
[42] X. Lin, S. Ji, X. Qiao, H. Hu, N. Chen, Y. Dong, Y. Huang, D. Guo, P. Tu, M. Ye, Density functional theory calculations in stereochemical determination of terpecurcumins J-W, cytotoxic terpene-conjugated curcuminoids from Curcuma longa L, J. Org. Chem., 78 (2013) 11835-11848.
[43] H.Z. Hu, Q. Gu, C. Wang, C.K. Colton, J. Tang, M. Kinoshita-Kawada, L.Y. Lee, J.D. Wood, M.X. Zhu, 2-aminoethoxydiphenyl borate is a common activator of TRPV1, TRPV2, and TRPV3, J. Biol. Chem., 279 (2004) 35741-35748.
[44] P. Yu, J. Li, J. Jiang, Z. Zhao, Z. Hui, J. Zhang, Y. Zheng, D. Ling, L. Wang, L.H. Jiang, J. Luo, X. Zhu, W. Yang, A dual role of transient receptor potential melastatin 2 channel in cytotoxicity induced by silica nanoparticles, Sci. Rep., 5 (2015) 18171.
[45] J. Hu, C. Lv, Z. Liu, L. Zhang, Cheminformatics analysis of the Chinese National Compound Library of Peking University, J. Chin. Pharm. Sci., 25 (2016) 669-675.

- Novel series of 2,3-dihydroquinazolin-4(1*H*)-one derivatives were designed and synthesized.
- Inhibitory activities targeting to the TRPM2 channel were evaluated by calcium imaging and electrophysiology approaches.
- Highly selective and active extracellular inhibitors of TRPM2 channel have been discovered.
- Structure-activity relationship was summarized.